ICHNOFOSSIL ASSEMBLAGES AND PALAEOSOLS OF THE UPPER TRIASSIC CHINLE FORMATION, SOUTH-EASTERN UTAH (USA): IMPLICATIONS FOR DEPOSITIONAL CONTROLS AND PALAEOCLIMATE

Sean J. FISCHER[1] & Stephen T. HASIOTIS[1]

[1]*Department of Geology, University of Kansas, 1475 Jayhawk Blvd., Lawrence, Kansas, 66045, USA;*
e-mails: seanfischer17@gmail.com, hasiotis@ku.edu

Abstract: The Upper Triassic Chinle Formation in the Stevens Canyon area in south-eastern Utah represents fluvial, palustrine, and lacustrine strata deposited in a continental back-arc basin on the western edge of Pangea. Previous investigations interpreted a megamonsoonal climate with increasing aridity for the Colorado Plateau towards the end of the Triassic. In this study, we systematically integrate ichnological and pedological features of the Chinle Formation into ichnopedofacies to interpret palaeoenvironmental and palaeoclimatic variations in the north-eastern part of the Chinle Basin. Seventeen ichnofossil morphotypes and six palaeosol orders are combined into twelve ichnopedofacies, whose development was controlled by autocyclic and allocyclic processes and hydrology. Ichnopedofacies are used to estimate palaeoprecipitation in conjunction with appropriate modern analogue latitudinal and geographic settings. In the north-east Chinle Basin, annual precipitation was ~1100–1300 mm in the Petrified Forest Member. Precipitation levels were >1300 mm/yr at the base of the lower Owl Rock Member, decreased to ~700–1100 mm/yr, and then to ~400–700 mm/yr. Two drying upward cycles from ~1100 mm/yr to ~700 mm/yr occurred in the middle and upper part of the Owl Rock Member. In the overlying Church Rock Member, precipitation decreased from ~400 mm/yr at the base of the unit to ~25–325 mm/yr at the end of Chinle Formation deposition. Ichnopedofacies indicate monsoonal conditions persisted until the end of the Triassic with decreasing precipitation that resulted from the northward migration of Pangea. Ichnopedofacies in the north-east Chinle Basin indicate both long-term drying of climate and short-term, wet-dry fluctuations.

Key words: Continental, trace fossils, groundwater profile, ichnology, ichnocoenoses, ichnopedofacies, Mesozoic.

INTRODUCTION

Analyses of ichnofossils and palaeosols provide a wealth of hydrological and climatic information in continental sedimentary deposits (e.g., Driese and Foreman, 1992; Turner, 1993; Hasiotis and Dubiel, 1994; Driese *et al.*, 1995; Birkeland, 1999; Kraus, 1999; Retallack, 2001; Driese and Mora, 2002; Prochnow et al., 2006a; Hasiotis *et al.*, 2007a, Cleveland *et al.*, 2008a; Dubiel and Hasiotis, 2011; Hasiotis and Platt, 2012). This study combines lithofacies, palaeosols, and ichnocoenoses of the Upper Triassic Chinle Formation (Fm) into ichnopedofacies to interpret palaeoenvironmental conditions and palaeoclimatic changes in the north-east Chinle Basin. These interpretations, in turn, will enable more detailed reconstructions of the variability in sedimentation rate, tectonics, and climate across the basin, building a more accurate regional picture of the Chinle

Fm through the Late Triassic. This is the first study to systematically integrate ichnological and pedogenic features in the Chinle Fm to determine local controls on base level, sediment deposition, pedogenesis, groundwater profile, and environments.

Palaeosols record the relative influence of soil-forming factors – climate, organisms, topography, parent material, and time (Jenny, 1941) – that modified sediments deposited on ancient landscapes (e.g., Retallack, 2001; Hasiotis, 2004, 2008; Hasiotis and Platt, 2012). Ichnofossils form through the interaction of organisms with a medium to produce three-dimensional structures influenced by such physiochemical factors as sedimentation rate, depositional energy, groundwater profile, nutrients, and oxygenation (Hasiotis, 2007; Hasiotis *et al.*, 2007a; Hasiotis and Platt,

2012). Combinations of these factors, unique to different depositional settings, are indicated by ichnocoenoses (ichnocoenosis, singular), co-occurring ichnofossil assemblages representing an ancient biological community interacting with the environment (Hasiotis *et al.*, 2012; Hasiotis and Platt, 2012), that are useful for identifying continental subenvironments (e.g., Hasiotis, 2004, 2008; Hasiotis *et al.*, 2007a, 2012; Smith *et al.*, 2008b; Hasiotis and Platt, 2012). Combining ichnology and palaeopedology to develop ichnopedofacies models — associations of ichnocoenoses and pedogenic features (Hasiotis *et al.*, 2007a) — allows for higher resolution interpretations of physiochemical conditions and soil-forming factors in the north-east Chinle Basin during the Late Triassic.

Pedological and ichnological studies in the Chinle Fm have been limited in scope. Local investigations of Chinle Fm palaeosols have concentrated in the centre of the Chinle Basin around the Petrified Forest National Park (PFNP; e.g., Kraus and Middleton, 1987a; Therrien and Fastovsky, 2000; Trendell *et al.*, 2012, 2013a, b; Atchley *et al.*, 2013), with other studies in northern New Mexico (Cleveland *et al.*, 2007, 2008a, b), western Colorado (Dubiel *et al.*, 1992), and eastern Utah (Prochnow *et al.*, 2005, 2006a, b). Much of this research utilized palaeosols to interpret fluvial architecture and sequence stratigraphy, showing that local fluvial evolution, topographic position, and salt tectonics had as great an, or even greater, influence on sedimentation and pedogenesis as did regional climate (e.g., Kraus and Middleton, 1987a; Prochnow *et al.*, 2005, 2006b; Cleveland *et al.*, 2007; Trendell *et al.*, 2012, 2013a). Few palaeosol studies in the Chinle Fm, though, have been combined with ichnological observations beyond plant ichnofossils (e.g., Dubiel *et al.*, 1992; Cleveland *et al.*, 2008a; Dubiel and Hasiotis, 2011; Ash and Hasiotis, 2013). Despite numerous descriptions of ichnofossils from PFNP (e.g., Hasiotis and Dubiel, 1993a, b, 1995a, b; Martin and Hasiotis, 1998; Hasiotis and Martin, 1999), research beyond this area of the basin is limited (e.g., Hasiotis and Mitchell, 1993; Hasiotis *et al.*, 1993; Hasiotis and Dubiel, 1994; Hasiotis, 1995; Gaston *et al.*, 2003; Gillette *et al.*, 2003), and few studies have established detailed local ichnocoenoses (Hasiotis and Dubiel, 1993b). More thorough studies combining ichnological and palaeopedological observations are imperative to interpret fine-scale climatic conditions across the Chinle Basin.

The main objectives of this study are to: 1) determine the variation of depositional systems and palaeoenvironmental settings; 2) establish ichnopedofacies and physiochemical conditions; and 3) interpret fine-scale (within member)

climatic conditions in the north-eastern Chinle Basin and compare it to the regional palaeoclimate of the south-western United States. This type of detailed sedimentological study is needed to more accurately interpret the spatial and temporal differences in sediment deposition, continental subenvironments, and climate between the edge and centre of the Chinle Basin during the Late Triassic.

GEOLOGIC SETTING

The Upper Triassic Chinle Fm was deposited in a continental back-arc basin on the western edge of Pangea between 5–30° N palaeolatitude (Fig. 1A; Van der Voo *et al.*, 1976; Dickinson, 1981; Parrish and Peterson, 1988; Bazard and Butler, 1991). Pangea migrated north during Chinle Fm deposition and the Colorado Plateau region reached 30° N palaeolatitude by the Early Jurassic (e.g., Dubiel and Hasiotis, 2011). The dominant drainage was to the north-west, and palaeoriver systems sourced from the Ouachita orogen in Texas flowed through both the Dockum and Chinle basins (Dubiel, 1994; Riggs *et al.*, 1996; Dickinson and Gehrels, 2008; Dubiel and Hasiotis, 2011). Sediment sources were the Uncompaghre Uplift, Amarillo-Wichita Highlands, and a magmatic arc on the western coast of Pangea that also supplied ash to the basin (Fig. 1A; e.g., Stewart *et al.*, 1972, 1986; Blakey and Gubitosa, 1983). Concurrent salt tectonism in the Salt Anticline Region of eastern Utah and western Colorado locally affected fluvial architecture, depositional geometries, and palaeosol development (Cater, 1970; Hazel, 1994).

The Chinle Fm consists of, in ascending order, the Shinarump (SM), Monitor Butte (MB), Moss Back (MM), Petrified Forest (PFM), Owl Rock (ORM), and Church Rock (CRM) members, and has a maximum thickness of over 500 m in the southern Four Corners area, thinning to the north-west and north-east (Fig. 1D; Stewart *et al.*, 1972; Dubiel, 1987, 1989; Dubiel *et al.*, 1989; Dubiel, 1994). Chinle Fm strata are separated from the Lower to Middle (?) Triassic Moenkopi Fm by the T-3 unconformity across the majority of the Colorado Plateau, and unconformably overlie the Lower Permian DeChelly Sandstone in northern Arizona (Stewart *et al.*, 1972; Pipiringos and O'Sullivan, 1978; Dubiel and Hasiotis, 2011). The J-0 unconformity marks the boundary between the Chinle Fm and the overlying Lower Jurassic Wingate Sandstone (Pipiringos and O'Sullivan, 1978; Dubiel, 1994; Hazel, 1994).

During the Late Triassic, deposition in the Chinle Basin was influenced by a megamonsoonal climate with wet and

Fig. 1. Palaeogeography, stratigraphy and location of the study area in south-eastern Utah (USA). **A.** Palaeogeography map, major patterns of fluvial systems and sediment transport, and tectonic setting of the Western Interior during Chinle Fm deposition (modified from Dickinson, 1981; Blakey, 1989; Dubiel, 1989, 1994; Riggs et al., 1996). Red star marks the study area. **B.** Field location map in south-eastern Utah. Red box is location of map shown in C. **C.** Map of Stevens Canyon, Indian Creek Canyon, and Canyonlands National Park. **D.** Generalized stratigraphic column of Chinle Fm in south-eastern Utah, with major unconformities. Red box outlines the members studied. White balloons are measured sections: S1 – Stick section 1, S2 – Stick section 2, S3 – Stick section 3, S4 – Stick section 4, S5 – Stick section 5, S6 – Stick section 6, SW – south-west measured section, W – west measured section, E – east measured section. **E.** Stevens Canyon at S1: Moss Back Member (MM), Petrified Forest Member (PFM), Owl Rock Member (ORM), Church Rock Member (CRM); Chinle Fm overlain by Wingate Sandstone (Wg).
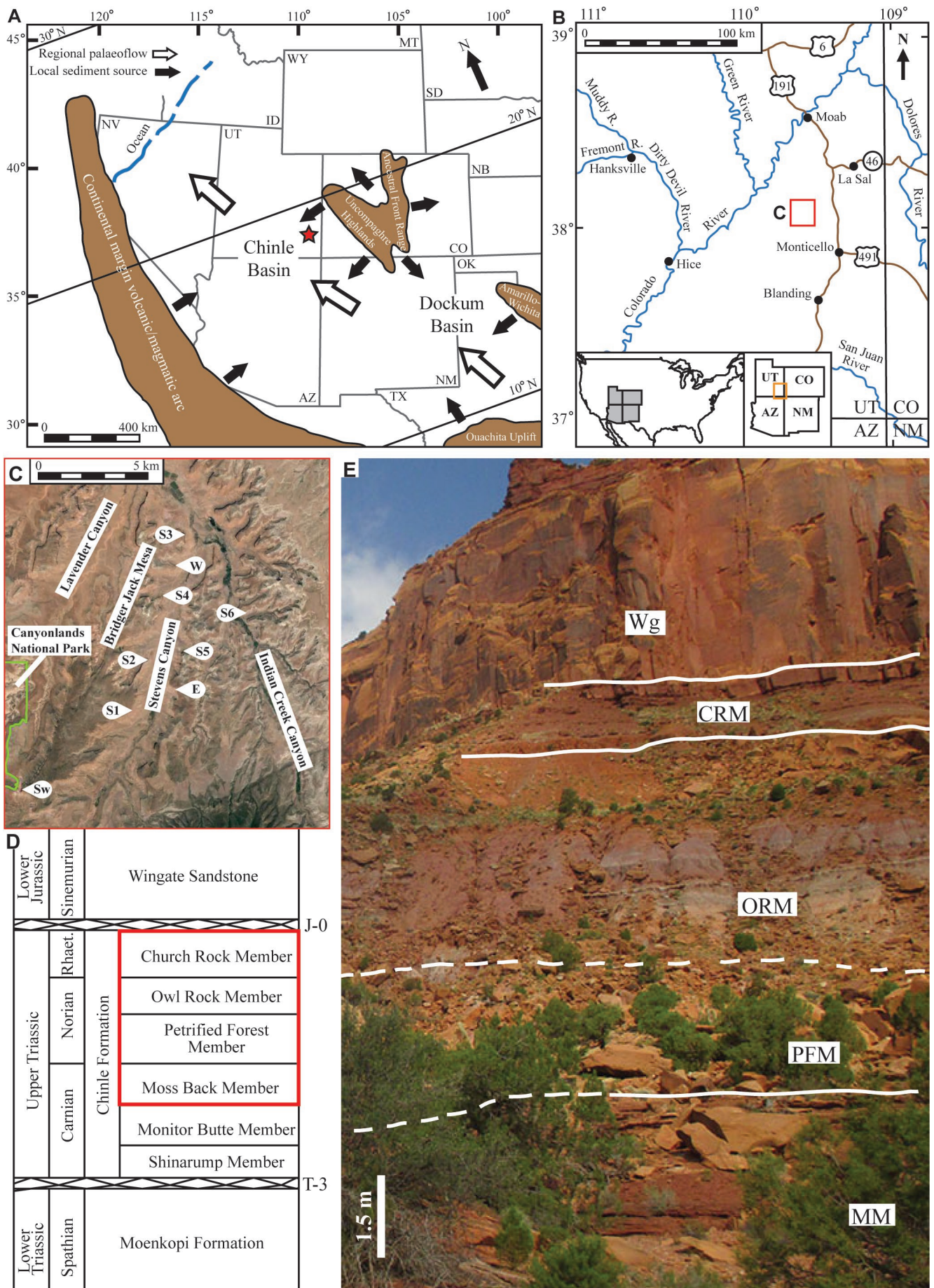
Fig. 1.

dry periods (Parrish and Peterson, 1988; Dubiel *et al.*, 1991; Dubiel, 1994; Dubiel and Hasiotis, 2011). Conditions became more arid towards the end of Chinle Fm deposition, represented by eolian sand sheet and playa lake strata in the CRM and equivalent Rock Point Member (RPM) (Dubiel, 1989; Dubiel *et al.*, 1991; Dubiel and Hasiotis, 2011). Chinle Fm sediments were eventually buried by migrating sand dunes of the Lower Jurassic Wingate Sandstone (Blakey and Gubitosa, 1983; Parrish and Peterson, 1988; Dubiel, 1989). The transition to drier conditions reflects the northward migration of Pangea towards the mid-latitudes (Dubiel, 1994; Cleveland *et al.*, 2008b; Dubiel and Hasiotis, 2011).

Study area

The study area is 56 km south of Moab, Utah, near the south-eastern border of Canyonlands National Park in Stevens Canyon and Indian Creek Canyon (Fig. 1B, C). The Upper Triassic Chinle Fm is locally represented by the MB, MM, PFM, ORM, and CRM (Fig. 1E). The top of the Chinle Fm is overlain by the Lower Jurassic Wingate Sandstone (Hasiotis and Mitchell, 1993; Hasiotis *et al.*, 1993).

The MB overlies and locally fills palaeochannels incised into the SM and unconformably overlies the Moenkopi Fm (Stewart *et al.*, 1972; Dubiel and Hasiotis, 2011). Only the top of the MB is present in one section and consists of red, yellow, and green-grey mudstone. Volcanic ash is a significant component of sediment, as evidenced by increased amount of bentonite, altered lithic clasts, and relict glass shards. The MB is interpreted as a complex mosaic of meandering fluvial, palustrine, lacustrine, and deltaic environments (Blakey and Gubitosa, 1983; Dubiel and Hasiotis, 2011).

The MM is preserved within the Cottonwood Palaeovalley, which incised into the underlying MB and Lower Triassic Moenkopi Fm (Stewart *et al.*, 1972; Blakey and Gubitosa, 1983; Dubiel and Hasiotis, 2011). Strata consist of brown to grey, medium-grained sandstone and carbonate-nodule conglomerate. Sandstones contain tabular-planar and trough-cross-stratification (TCS), large-scale lateral accretion, and rarer horizontal lamination, and sand-bodies consist of stacked, interconnected, broad sand sheets. Depositional environments are interpreted as braided fluvial systems (Blakey and Gubitosa, 1983, 1984; Dubiel, 1989; Dubiel *et al.*, 1991; Dubiel and Hasiotis, 2011).

The PFM overlies the MB and MB (Stewart *et al.*, 1972; Dubiel and Hasiotis, 2011). Lithofacies consist of lavender and brown, bentonitic sandstone and variegated, carbonate-nodule-bearing mudstone. Sandstones display TCS and lateral accretion, contain thin carbonate-nodule conglomerate lenses, and occur as ribbon and narrow sheet sand bodies encased in mudstone (Blakey and Gubitosa, 1984; Dubiel, 1987, 1989). Volcanic ash is a significant component of clastic sediment. The PFM was deposited in palustrine and high-sinuosity, suspended-load fluvial environments (Blakey and Gubitosa, 1983; Dubiel, 1987; Dubiel *et al.*, 1991).

The ORM overlies the PFM. Lithofacies consist of orange and red siltstone (Stewart *et al.*, 1972; Dubiel, 1987).

Intraformational carbonate-nodule conglomerate lenses derived from adjacent palaeosols are present and display large-scale, lateral accretion (e.g., Dubiel and Hasiotis, 2011). The ORM was deposited in fluvial and lacustrine environments (Blakey and Gubitosa, 1983; Dubiel, 1994; Dubiel and Hasiotis, 2011).

The CRM overlies the ORM. Lithofacies consist of red, orange, and brown siltstone and sandstone, with sandstone occurring as broad sheet and ribbon sand bodies with TCS, ripple-cross-lamination, horizontal lamination, and lateral accretion (Stewart *et al.*, 1972; Blakey and Gubitosa, 1983, 1984; Dubiel, 1989; 1994). The CRM was deposited in fluvial and playa lake environments (e.g., Dubiel, 1987; Dubiel *et al.*, 1991).

METHODS AND MATERIALS

Eight sections (Fig. 2) were measured using a 1.5-m-long Jacobs Staff. Sedimentary facies description included unit thickness, colour, grain size, grain type, degree of sorting, sedimentary structures, and bedding morphology (e.g., Compton, 1985). Lithofacies were separated according to grain size, and further subdivided based on dominant sedimentary structures (e.g., Miall, 1996; van der Kolk et al., 2015). Facies associations were assigned according to Collinson (1986) and Miall (1996). Chinle Fm units were correlated by walking out lithofacies associations at the outcrop and by tracing them out from panoramic photos.

Ichnofossils were described by their architectural and surficial morphology, and internal fill (Hasiotis and Mitchell, 1993; Hasiotis *et al.*, 1993; Bromley, 1996). Ichnofossils were assigned to a category of burrowing behaviour that reflects spatial position and moisture zone in the soil profile (Hasiotis, 2000, 2004, 2008; Hasiotis *et al.,* 2007). Epiterraphilic behaviour is displayed by ichnofossils constructed on the surface of the soil profile and include trackways. Terraphilic behaviour is reflected by ichnofossils constructed above the water table near the surface of the soil-water profile and in the upper vadose zone where soils are well drained overall. Hygrophilic behaviour reflects burrow construction above the water table in the upper, intermediate, and lower vadose zone. Ichnofossils constructed in fully saturated conditions at or beneath the water table in the phreatic zone, or beneath the sediment surface in open bodies of water, display hydrophilic behaviour. Specific ichnogenera (or ichnofossils) can be assigned to more than one category. Ichnocoenoses were determined through immediate horizontal and vertical associations of ichnofossils along stratigraphic horizons, and named according to the dominant ichnogenus (or ichnofossil) present.

Palaeosols were described according to Mack *et al.* (1993), Kraus (1999), and Retallack (2001). Pedogenic observations included matrix colour, mottling colour, horizonation, soil structures, slickensides, and calcium carbonate nodules. Colour was determined from fresh exposure using Munsell soil colour (Munsell Soil Colour Book, 2009). Palaeosol profiles were subdivided by horizons and designated as A (upper; zone of eluviation), B (intermediate; zone of illuviation), and C (lowest; parent material) (e.g., Retallack, 2001; Hasiotis *et al.*, 2007a);
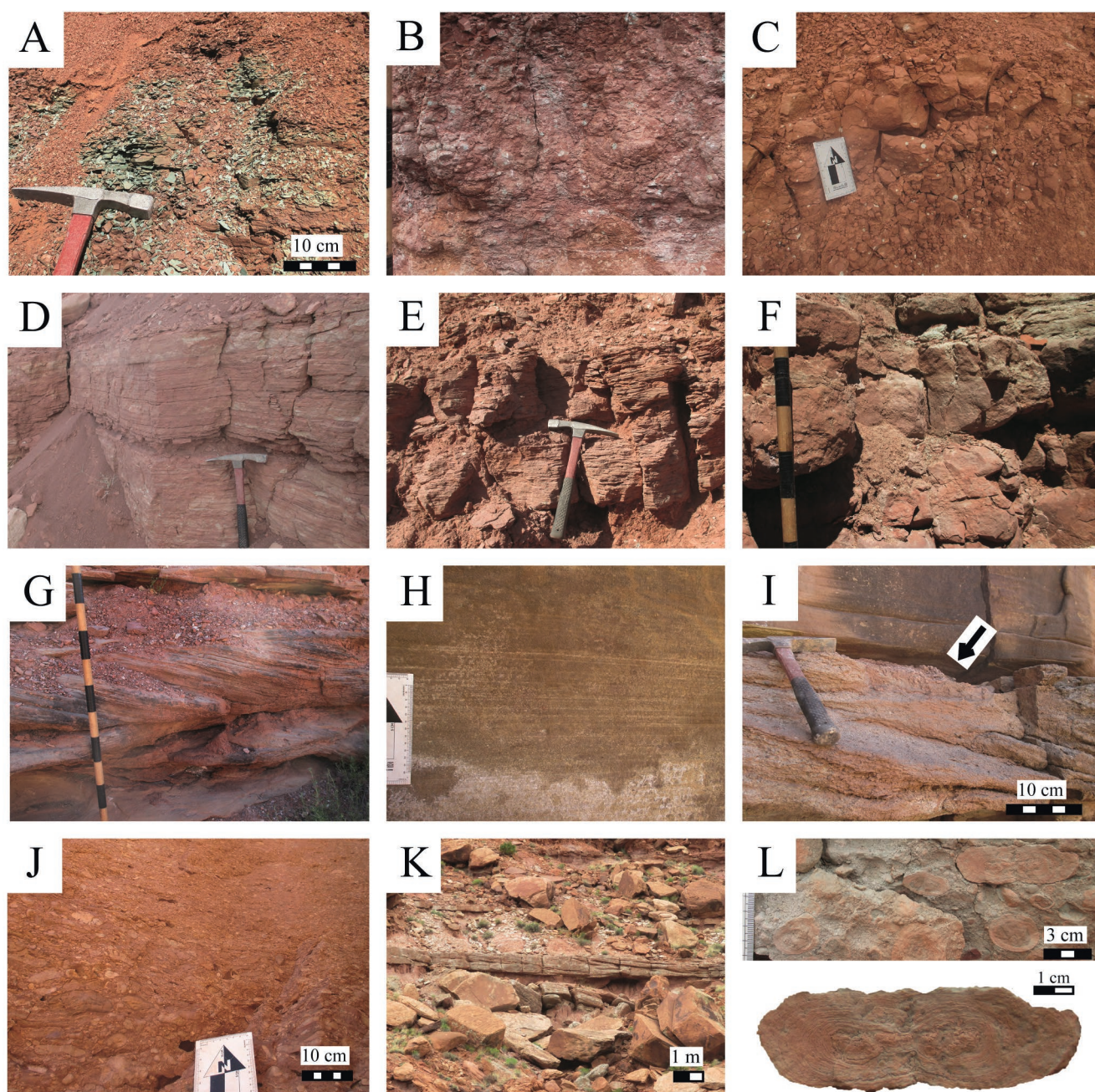
Fig. 2. Lithofacies of Chinle Fm. Staff in 10-cm intervals. Grain size card 15 cm tall. Rock hammer 33 cm long. **A.** Massive to finely laminated mudstone (F-1). **B.** Massive siltstone (F-2a). **C.** Massive siltstone to very fine-grained sandstone (F-2b). **D.** Planar-laminated siltstone to very fine-grained sandstone (F-2c). **E.** Ripple cross-laminated siltstone to very fine-grained sandstone (F-3). **F.** Massive fine- to very coarse-grained sandstone (F-4a). **G.** Trough cross-stratified (TSC) fine- to coarse-grained sandstone (F-4b). **H.** Planar-laminated fine- to coarse-grained sandstone (F-4c). **I.** TCS conglomerate (arrow) (F-5a). **J.** Massive to planar-laminated conglomerate (F-5b). **K.** Incline-bedded conglomerate (F-5c). **L.** Close-up of incline-bedded conglomerate showing pebble-sized quartz and limestone clasts. Large oncoid clast from incline-bedded conglomerate.

horizons can have shared designations based on pedogenic features present (e.g., AB, BC, AC). Calcium carbonate stages of accumulation (designated by k) were described according to Gile *et al.* (1966) and Machette (1985). Palaeosols were classified as entisols if primary sedimentary structures were present (Hasiotis *et al.*, 2007a; Dubiel and Hasiotis, 2011). Inceptisols and calcic inceptisols were identified as weakly developed with incipient horizonation and calcium carbonate accumulation (*sensu* Mack *et al.*, 1993)

similar to stages 1–2 of calcic horizon development (Gile *et al.*, 1966; Machette, 1985). Inceptisols were differentiated from entisols by a lack of primary sedimentary structures. Vertisols were identified by slickensides, prismatic peds, and redoximorphic colouration (Dubiel and Hasiotis, 2011). Alfisols and calcic alfisols were defined as palaeosols with elevated clay horizons (*sensu* Mack *et al.*, 1993) and carbonate accumulation similar to stages 2–3 of calcic horizon development (Gile *et al.*, 1966; Machette, 1985).

Ichnopedofacies were constructed based on the combined vertical and lateral associations of sedimentary facies, ichnofossils, and pedological features (Hasiotis *et al.*, 2007a). First, the dominant sedimentary facies were described. Then, horizons were differentiated and the palaeosol order was determined. Next, features of the dominant ichnocoenosis present were incorporated into the pedogenic diagnosis. From this, ichnopedofacies were named by combining the names of the dominant ichnocoenosis and palaeosol (if present) comprising the unit.

In the laboratory, 22 thin sections (7.62 × 5.08 cm) impregnated with blue epoxy were observed under a Nikon Eclipse™ E600 POL petrographic polarizing light microscope (1–40×) with attached digital camera for lithological description. Pedological micromorphology was described according to Brewer (1976). Rock samples were also observed under a Nikon SMZ™ 1000 binocular scope (1–8×) for lithological and ichnological description. Descriptions from microscope supplemented field observations and aided classification of sedimentary facies, ichnocoenoses, and palaeosol orders.

Samples were crushed to under 150 μm for X-ray diffraction (XRD) and X-ray fluorescence (XRF) analysis. XRD was performed on 76 samples at the University of Kansas Small Molecule X-Ray Crystallography Lab using a Bruker MicroSTAR™ diffractometer. Qualitative mineralogical data was collected with a scan rate of three, one-minute runs from 5–115° 2θ. Clay mineralogy was determined according to Moore and Reynolds (1997). XRD data was used to determine the clay mineralogy of palaeosols and to aid the identification of clay-rich horizons marking alfisols and calcic alfisols. XRF was conducted at Oneida Research Services on 30 samples to determine elemental weight percentages; values were mathematically converted to weight percent oxide and molar ratios. XRF data was used to track changes in elemental composition in palaeosol profiles and to differentiate palaeosol horizons, especially calcic horizons. Both XRD and XRF data aided in amending palaeosol classifications made in the field.

RESULTS

Lithofacies

Five distinct lithofacies consisting of 11 subfacies were identified from outcrop (Table 1). Mudstone facies contain units composed predominately of mud-sized grains and were not subdivided into subfacies. Siltstone subfacies were subdivided based on the presence of planar lamination and the relative amount of very fine sand grains (Fig. 2). Sandstone and conglomerate subfacies were separated based on the dominant primary sedimentary structures (Fig. 2).

Ichnology

Seventeen ichnogenera and ichnofossils were identified (Table 2; Fig. 3). These ichnofossils form nine reoccurring ichnocoenoses across the north-east Chinle Basin (Table 3). We maintain the use of *Steinichnus* (i.e., *S. carlsbergi*; Bromely and Asgaard, 1979) and reject the synonymy of

it with *Spongeliomorpha* (Melchor *et al.*, 2009). We base our position on morphological criteria that distinguishes *Steinichnus* from *Spongeliomorpha*. *Spongeliomorpha* is the morphological version of *Ophiomorpha* and *Thalassinoides*, but with strongly longitudinal scratches, in which all three ichnogenera exhibit a three-dimensional box work or maze work of interconnected shafts and tunnels with widened areas were the tracemaker can turn around, differing only in the use of pellets as a wall lining, no wall lining, and scratches (i.e., *Spongeliomorpha*). *Steinichnus* does not exhibit any of these morphological features or criteria. Instead it is a horizontal, flattened cylinder (oval in cross-section) with secondary (produced by another tracemaker using the same tunnel but going in another direction to form an apparent branch) and pseudobranching (produced by a cross-cutting burrow of the same or similar morphology), with strongly transverse to weakly longitudinal striations on the floor and sides of the burrow wall with no fill or chaotic fill of the burrow; the top of the burrow may be pustoluse or knobby and show no scratches (Bromley and Asgaard, 1979; Hasiotis, 2002; Bohacs *et al.*, 2007; Smith *et al.*, 2009). Thus, we consider *Steinichnus* and *Spongeliomorpha* to be two distinctly different ichnogenera with unique morphological features.

Palaeosols

Six types of palaeosols were identified by pedogenic development: entisols, inceptisols, vertisols, calcic inceptisols, alfisols, and calcic alfisols (Table 4). Every member of the Chinle Fm shows some degree of pedogenic modification.

Entisols: Profiles consist of compound AC and C horizons. Roots and burrows penetrate parent material, which display primary sedimentary structures. Entisols contain the highest variety of ichnocoenoses, but most consist of horizontal, shallow burrows (Tables 3, 4). Entisols are present in the MM, PFM, ORM, and CRM.

Inceptisols: These have compound, composite, and cumulative A-C and AC profiles. Inceptisols are observed in the PFM, ORM, and CRM.

Calcic inceptisols: These consist of composite ABk, A-ABk-AB, A-AB-ABk, and A-AB-Bk-C profiles. ABk and Bk horizons are 55–95 cm thick and reach stages 1–2 of calcic palaeosol development. Carbonate accumulation manifests as nodules 5–8 mm in diameter; horizons have weight percent CaO from 51.78%–99.50%. Calcic horizons commonly overprint each other to form composite palaeosol profiles. Calcic inceptisols are present in the PFM, ORM, and CRM.

Vertisols: These consist of compound to cumulative A-Bss profiles. Strong redoximorphic mottling is present in Bss horizons. Vertisols occur only in the ORM.

Alfisols: These consist of composite and cumulative A-Bt and A-AB-Bt profiles. Bt horizons are characterized by illite and montmorillonite. Alfisols occur only in the ORM.

Calcic alfisols: These consist of composite A-Btk and A-Bt-Btk profiles. Bt horizons are characterized by illite and montmorillonite and increased calcium accumulations. Btk horizons are 0.12–3 m thick and contain illite and montmorillonite. Calcium carbonate accumulation match stages 2–3

Table 1

Chinle Formation lithofacies.

Facies	Lithology	Thickness	Sediment grain size and texture	Composition
F-1	Massive to finely laminated, red, pale red, brown, and green-grey mudstone	0.3–4.75-m	Mud with rare silt and very fine sand; subangular to subrounded; moderately to well-sorted	Mud; silt and sand grains comprised of quartz and calcite; calcium carbonate cement
F-2a	Massive red, pale red, and green-grey siltstone	0.02–12.0-m	Silt with mud and very fine sand; grains angular to subrounded; moderately to well-sorted	Silt and sand grains comprised of quartz, calcite, and siltstone clasts; variable mud between grains; Fe and Mn nodules ranging from <0.1-mm to 0.3-mm in diameter; calcium carbonate cement
F-2b	Massive, red, pale red, and brown siltstone to sandstone	0.1–5.4-m	Silt with very fine sand and mud; subangular to subrounded; moderately to well-sorted	Silt and sand grains comprised of quartz, calcite, siltstone clasts, and rare muscovite; variable mud between grains, Fe and Mn nodules <0.1-mm in diameter; calcium carbonate cement
F-2c	Planar-laminated, red, pale red, and brown siltstone to sandstone	0.02–2.5-m	Silt with very fine sand and mud; angular to subrounded; moderately to well-sorted	Silt and sand grains comprised of quartz, calcite, and siltstone clasts; variable mud between grains, often draped along laminations; Fe and Mn nodules <0.1-mm in diameter; calcium carbonate cement
F-3	Ripple-cross-laminated, red, pale red, brown, and green-grey siltstone to sandstone	0.02–7.5-m	Very fine to medium sand with silt and mud; subangular to subrounded; moderately to well-sorted	Silt and sand grains comprised of quartz, calcite, siltstone clasts, and rare muscovite; variable mud between grains, often draped along laminations; Fe and Mn nodules <0.1-mm in diameter; calcium carbonate cement
F-4a	Massive, red, brown, and green-grey sandstone	0.1–2.0-m	Fine to very coarse sand; subrounded to rounded; well-sorted	Sand grains comprised of quartz, siltstone clasts, lithic fragments, and limestone clasts; Fe and Mn nodules <0.1-mm in diameter; calcium carbonate cement
F-4b	Trough-cross-stratified, brown sandstone	0.9–2.0-m	Very fine to coarse sand; grains subrounded to angular; moderately sorted	Sand grains comprised of quartz, lithic clasts, muscovite, and feldspar; quartz grains show overgrowth cement; Fe and Mn nodules <0.1-mm in diameter
F-4c	Planar-laminated, brown, and green-grey sandstone	0.04–6.7-m	Fine to coarse sand with silt and mud; subangular to rounded; moderately to well-sorted	Sand and silt grains comprised of quartz, siltstone clasts, lithic fragments, and limestone clasts; variable mud and siltstone between sand grains; Fe and Mn nodules <0.1-mm in diameter; calcium carbonate cement
F-5a	Trough-cross-stratified, brown and green-grey conglomerate	0.2–2.1-m	Granule to cobble clasts; poorly sorted	Quartz, lithic, and limestone clasts; Fe nodules <0.1-mm in diameter
F-5b	Massive to planar-laminated, red, brown, and green-grey conglomerate	0.01–2.1-m	Granule to pebble clasts; poorly sorted	Quartz, siltstone, lithic, and limestone clasts; calcium carbonate cement
F-5c	Incline-bedded, brown and green-grey conglomerate	0.75-m	Granule to pebble clasts; poorly sorted; beds graded and show lateral accretion	Quartz, limestone, and lithic clasts, oncoids up to 3.5-cm x 12-cm in diameter

Table 2

Chinle Formation ichnofossils. Abbreviations of stratigraphic units: CRM – Church Rock Member; ORM – Owl Rock Member; PFM – Petrified Forest Member.

Ichnofossil	Size	Description	Interpretation	Behavior	Stratigraphic position
Arenicolites	openings 2–7-mm diameter, 2–10-mm apart	Vertical, cylindrical shafts connected by a horizontal cylindrical tunnel to form a U-shape; paired cylindrical openings; smooth walls; convex epirelief	Morphology typical of U-shaped, freshwater mayfly burrows (e.g., Wallace and Merritt, 1980; Kureck, 1996; Hasiotis, 2002, 2004, 2008)	Hydrophilic	ORM
Ancorichnus	4-mm diameter	Horizontal tunnels with smooth wall linings and meniscate backfill; tunnels do not branch; concave and convex epirelief	Morphology typical of Mesozoic continental examples; beetle larvae? (e.g., Frey *et al.*, 1984; Hasiotis, 2002, 2004, 2008; Smith *et al.*, 2008a)	Hygrophilic	ORM
Camborygma	0.6–12-cm diameter, up to 185-cm long	Vertical to subvertical, cylindrical to J-shaped shafts; branching and chamber development; walls lined or unlined; surficial scratch and scrape marks; full relief or concave epirelief	Morphology typical of present-day and ancient freshwater crayfish burrows (e.g., Hobbs, 1981; Hasiotis and Mitchell, 1993; Hasiotis *et al.*, 1993; Hasiotis and Honey, 2000; Smith *et al.*, 2008c)	Hydrophilic	PFM, ORM
Cylindricum	2–7-mm diameter	Vertical, test-tube-shaped shafts with rounded lower ends; cylindrical openings in map view; convex epirelief	Morphology typical of vertical insect burrows; various beetles (e.g., Stanley and Fagerstrom, 1974; Ratcliffe and Fagerstrom, 1980; Hasiotis, 2002)	Terraphilic	PFM, ORM, CRM
Fictovichnus	1.5-cm diameter, up to 3-cm long	Ovoid capsules; walls smooth or show high density pattern of transverse scratch marks; full relief	Morphology typical of present-day insect cocoons (e.g., Johnston *et al.*, 1996; Vittum *et al.*, 1999; Hasiotis, 2002, 2003; Counts and Hasiotis, 2009)	Terraphilic	ORM
Naktodemasis	0.5–6-mm diameter	Subvertical to subhorizontal, unlined, tunnels of meniscate-backfilled packages; meniscae thin, tightly spaced, ellipsoidal; tunnels straight to sinuous; unbranched; do not weather differentially from matrix	Burrow morphology similar to extant Scarabaeidae beetle larvae and Cicadidae nymph burrows in present-day soils (e.g., Hasiotis and Dubiel, 1994; Smith and Hasiotis, 2008; Smith *et al.*, 2008a, b; Counts and Hasiotis, 2009, 2014; Hasiotis, 2008)	Terraphilic, hygrophilic	PFM, ORM
Planolites	3–14-mm diameter	Horizontal to subhorizontal, simple, unlined, unbranched, cylindrical tunnels; cylindrical openings in cross section	Morphology typical of Paleozoic and Mesozoic examples (e.g., Pemberton and Frey, 1982; Hammersburg *et al.*, 2018)	Hydrophilic	All mbrs
Rhizocretions	2–7-cm diameter, up to 3-m long	Vertical, infilled shafts, taper towards bottom; infill same as matrix and/or CaCO3 nodules, cement; irregular bumpy surface; full relief	Morphology typical of present-day and ancient concretions around roots (e.g., Klappa, 1980; Hasiotis, 2002; Kraus and Hasiotis, 2006)	Terraphilic	PFM, ORM
Rhizohaloes	0.4–8-cm diameter, 1-m long	Vertical to subvertical halo surrounding root trace; original root material absent	Morphology typical of Mesozoic rhizohaloes (e.g., Hasiotis, 2002; Kraus and Hasiotis, 2006)	Terraphilic	All mbrs

Table 2 cont.

Chinle Formation ichnofossils. For abbreviations of stratigraphic units, see part 1 of this table.

Ichnofossil	Size	Description	Interpretation	Behavior	Stratigraphic position
Rhizoliths	1- to <7-mm diameter, up to 60-cm long	Vertical to subvertical, sinuous traces; dendritic branching; crosscut; taper towards base; can contain fragments of original root material and matrix filled	Morphology typical of present-day and ancient rhizoliths (e.g., Klappa, 1980; Retallack, 2001; Hasiotis, 2002, 2004, 2008; Kraus and Hasiotis, 2006; Smith et al., 2008b)	Terraphilic	All mbrs
Rhizotubules	6–9-cm diameter, 20–60-cm long	Vertical to subvertical, CaCO3, cylindrical, nodular tubes, branch, taper towards base	Morphology typical of present-day rhizotubules (e.g., Klappa, 1980; Kraus and Hasiotis, 2006)	Terraphilic	ORM
Scoyenia	1–6-mm diameter	Horizontal to subhorizontal, straight to sinuous, unlined, meniscate-backfilled tunnels; ropey texture of overlapping scratch marks; unbranched, crosscut; meniscate packages thin, tightly spaced; convex epirelief	Burrow morphology similar to extant burrows of beetle and dipteran larvae in soils and sediments (e.g., Frey et al., 1984; Hasiotis and Dubiel, 1995a; Hasiotis, 2002; Hasiotis et al., 2012)	Hygrophilic	PFM, ORM, CRM
Skolithos	2–5.5-mm diameter, 3.5–12-cm long	Vertical, simple, straight, cylindrical shafts; walls smooth	Morphology produced by multiple organisms (e.g., Hasiotis, 2002, 2004, 2008; Hasiotis et al., 2012)	Terraphilich hygrophilic	ORM
Steinichnus	4–9-mm diameter	Horizontal, cylindrical, sinuous tunnels; width varies across a single tunnel; branch and cross cut; structureless tunnel fill; convex epirelief	Burrow morphology similar to extant mud-loving beetle and mole cricket burrows (e.g., Ratcliffe and Fagerstrom, 1980; Bromley and Asgaard, 1979; Hasiotis, 2002; Hasiotis et al., 2012)	Hygrophilic	ORM
Tetrapod footprint	9–20-cm long, 4–11-cm deep	Only seen in cross section; footprint preserved as depressions that deform underlying bedding	Morphology typical of tetrapod tracks in Paleozoic and Mesozoic strata (e.g., Hasiotis, 2002; Hasiotis et al., 2007b)	Epiterraphilic	PFM, CRM
Therapsid burrow	6–16-cm diameter, 215-cm long	Vertical to subvertical, helical and cylindrical shafts; walls with V-shaped scratch marks; full relief	Morphology typical of therapsid burrows in Paleozoic and Mesozoic strata (e.g., Smith, 1987; Hasiotis et al., 2007b)	Terraphilic	PFM, ORM
Treptichnus	7-mm diameter	Horizontal tunnels with shallow, U-shaped segments that form a zig-zag or irregular pattern; forked where segments connect; convex epirelief	Dipteran larva or pupa trail searching for appropriate moisture level to complete pupation (e.g., Getty et al., 2016; Hammersburg et al., 2018)	Hygrophilic	ORM
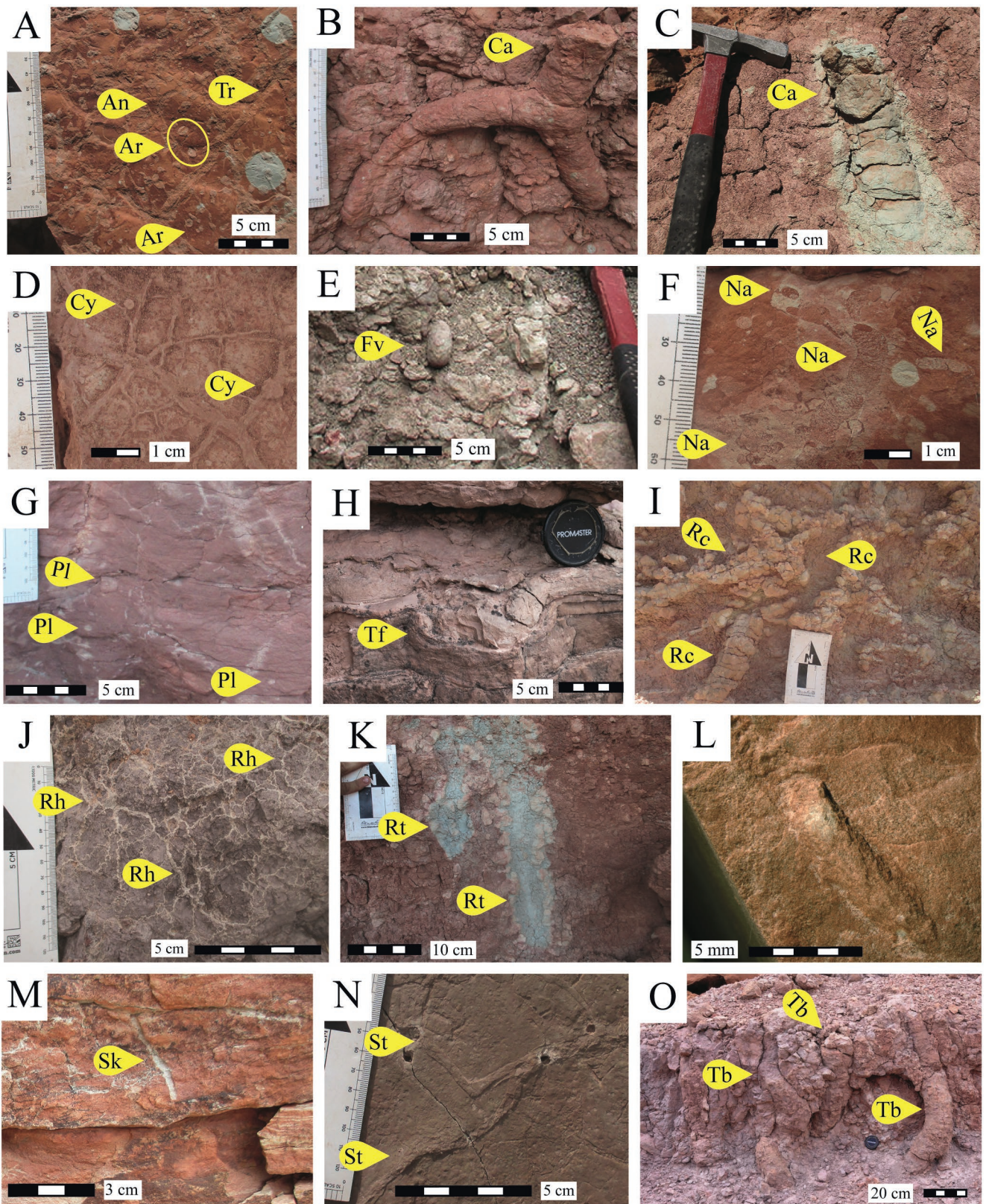
Fig. 3. Chinle Fm ichnofossils. Rock hammer 33 cm long **A.** *Ancorichnus* (An), *Arenicolites* (Ar), and *Treptichnus* (Tr). **B.** Branching form of *Camborygma* (Ca). **C.** *Camborygma* (Ca) with a straight, cylindrical morphology. **D.** *Cylindricum* (Cy). **E.** *Fictovichnus* (Fv). **F.** *Naktodemasis* (Nk). **G.** *Planolites* (Pl). **H.** Tetrapod footprint (Tf). **I)** Rhizocretion (Rc). **J)** rhizolith (Rh). **K.** Rhizotubule (Rt). **L.** *Scoyenia* (Sc). **M.** *Skolithos* (Sk). **N.** *Steinichnus* (St). **O.** Therapsid burrows (Tb).

Table 3

Chinle Formation ichnocoenoses. Ichnofossils listed in order of abundance.

Ichnocoenoses	Ichnofossils	Facies
I-1. *Camborygma*	*Camborygma, Naktodemasis*, rhizohaloes, and rhizoliths; rare therapsid burrows, *Scoyenia*, tetrapod tracks, *Cylindricum*, and *Skolithos*	F-2a, F-2b, F-2c, F-3, F-4a
I-2. *Cylindricum*	*Cylindricum* and *Scoyenia*	F-2c, F-3
I-3. *Naktodemasis*	*Naktodemasis*, rhizohaloes, rhizoliths; rare *Camborygma* and *Planolites*	F-2a, F-2b
I-4. *Naktodemasis–Camborygma*	*Naktodemasis, Camborygma*, rhizoliths, and *Scoyenia*; rare *Ancorichnus, Arenicolites, Cylindricum, Planolites*, and *Treptichnus*	F-2a, F-2b, F-3
I-5. Rhizolith	Rhizohaloes, rhizoliths, rhizocretions, rhizotubules; rare *Planolites, Naktodemasis*, and *Skolithos*	F-1, F-2a, F-2b, F-2c, F-3, F-4a
I-6. *Scoyenia*	*Scoyenia* and rhizoliths; rare *Cylindricum, Planolites*, and *Camborygma*	F-2a, F-3
I-7. *Skolithos*	*Skolithos*; rare *Planolites* and *Naktodemasis*	F-2c
I-8. *Steinichnus*	*Steinichnus*; rare rhizoliths	F-1, F-4b
I-9. Therapsid	Therapsid burrows, *Camborygma*, rhizohaloes, rhizoliths; rare *Cylindricum, Scoyenia*, and *Naktodemasis*	F-2a, F-2b

of calcic palaeosol development with nodules 0.5–2.0 cm in diameter; horizons have weight percent CaO of 66.64%––87.43%, Calcic alfisols only occur in the ORM.

Facies associations

Lithofacies, ichnocoenoses, and palaeosols form six re-occurring facies associations from proximal to distal position on the alluvial plain (Table 5; Fig. 4). FA-1 is most abundant in the MM and also abundant in the CRM, where TCS sandstone occurs as stacked, interconnected, laterally extensive sand sheets. FA-2 is most abundant in the middle ORM. Conglomerate beds have erosive bases and occur as thin, laterally discontinuous, ribbon sand bodies encased in siltstone; large oncoids are common as clasts. FA-3 is common in the ORM, consisting of stacks of interbedded massive siltstone, ripple-cross-laminated sandstone, and laterally discontinuous sandstone and conglomerate beds. FA-4 forms the majority of the PFM and ORM and is also observed in the CRM, and consists of fine siliciclastic facies. FA-5 is rarely observed in the PFM and ORM and consists of planar-laminated mudstone and siltstone with ichnofossils along bedding planes. FA-6 is only observed in the CRM, consists of planar-laminated siltstone and very fine sandstone, and is the least abundant facies association. FA-6 is differentiated from FA-5 by rare to absent ichnocoenoses and palaeosols.

Ichnopedofacies

Shallowly burrowed entisol (IPF I): Compound AC horizons with primary sedimentary structures within crevasse-splay and levee (FA-3) and palustrine (FA-5) deposits that contain at least one of these ichnocoenoses: *Cylindricum, Scoyenia, Skolithos*, or *Steinichnus* (Tables 3–5; Fig. 5A–C). The *Cylindricum* ichnocoenosis is common in planar- and ripple-cross-laminated siltstone to very fine sandstone (F-2c and F-3) with abundant desiccation cracks. The *Scoyenia* ichnocoenosis is mainly associated with massive siltstone (F-2a) and ripple-cross-laminated siltstone to fine sandstone (F-3). The *Skolithos* ichnocoenosis is associated with lens-shaped sandstone bodies that display planar-laminated bedding (F-2c), whose base is erosional with a thin bed of conglomerate and surrounded by fine-grained strata. The *Steinichnus* ichnocoenosis occurs in planar-laminated mudstone (F-1) with abundant desiccation cracks. Ichnofossils primarily occur along bedding planes and penetrate <12 cm into the sediment.

Rhizolith entisol (IPF II): Compound AC horizons with the rhizolith ichnocoenosis (Tables 3–5; Fig. 5D–F) in ripple-cross-laminated sandstone (F-3), massive medium sandstone (F-4a), and massive pebble conglomerate (F-5b) within braided-river (FA-1) and crevasse-splay and levee (FA-3) deposits. Ripple-cross-laminated sandstone commonly occurs above laterally extensive, stacked, TCS sandstone. Massive medium sandstone and pebble conglomerate bodies form thin, laterally extensive sheets with erosive bases. Red-brown rhizoliths and green-grey rhizohaloes occur along bedding planes associated with lithofacies F-4a and F-5b. Deeper penetrating green-grey rhizohaloes, 15–70-cm deep and 18–85-cm long, occur with *Planolites* in lithofacies F-3.

***Camborygma* entisol (IPF III):** Compound AC horizons and the *Camborygma* ichnocoenosis (Tables 3–5; Fig. 6A–C) in ripple-cross-laminated siltstone and sandstone (F-3), massive medium–coarse sandstone (F-4a), and massive pebble conglomerate (F-5b) within crevasse-splay and levee deposits (FA-3). Massive sandstones and conglomerates have thin, laterally extensive sheet morphologies. *Camborygma* is ≤0.5-m deep and long in massive, medium sandstone to pebble conglomerate. *Camborygma*

Table 4

Chinle Formation palaeosols.

Palaeosol order	Hori-zons	Munsell colours and codes	Common pedogenic features	Facies	Ichnoco-enoses
P-1. Entisol	AC, C	Red (10R 5/4, 2.5YR 5/6), pale red (10R 6/3, 6/2), red brown (2.5YR 4/3), and green grey (Gley 1 8/10GY); mottle colours of pale-red (10R 7/3), brown (2.5Y 7/3, 2.5YR 7/3), yellow (5Y 6/8, 2.5Y 7/8), and green-grey (Gley 1 7/10Y) reduction haloes	Primary bedding and sedimentary structures present; bedding disrupted by roots and burrows	F-2c, F-3, F-4a, F-4b	I-1, I-2, I-3, I-4, I-5, I-6, I-7, I-8
P-2. Inceptisol	A, AC, C	Red (10R 4/3, 2.5YR 4/6, 5/6) and red brown (2.5YR 3/4, 4/4); mottle colours of pale red (10R 6/3) and green-grey (Gley 1 7/10Y) reduction haloes	Weak horizon development; A horizon has angular blocky and granular peds	F-1, F-2a, F2b	I-3, I-5
P-3. Calcic inceptisol	A, AB, ABk, Bk, C	A—Red (2.5YR 4/5, 5/6), pale red (10R 6/2), red brown (5R 5/3, 4/4, 2.5YR 4/4), brown (7.5YR 4/2); mottle colours of red (10R 4/2), yellow (5YR 6/6, 10YR 7/3, 2.5YR 4/3), grey (10R 7/1) and green-grey (Gley 1 7/10Y, Gley 1 8/10GY) reduction haloes; AB—Red (10R 5/6) and red brown (10R 4/3); mottle colours of green-grey (Gley 1 7/10Y) reduction haloes; ABk, Bk—Red (10R 5/6, 2.5YR 5/4) and pale red (10R 4/3, 5/2); mottle colours of red (2.5R 3/6), pale red (10R 6/2), red-brown (2.5R 5/4), yellow (5YR 6/6, 10YR 7/3, 2.5YR 4/3) and green-grey (Gley 1 7/10Y) reduction haloes	A horizon has angular blocky and granular peds; AB horizon has angular blocky and granular peds, redder than overlying A horizon; ABk and Bk horizons have angular blocky and granular peds, Stages 1–2 calcium carbonate accumulation; green-grey reduction haloes	F-2a, F-2b	I-1, I-3, I-9
P-4. Vertisol	A, Bss	A—Pale red (5R 5/3); yellow (2.5Y 7/4) rhizohaloes; Bss—Pale red (5R 5/3) and green grey (Gley 1 7/10GY)	A horizon has angular blocky and prismatic peds; Bss horizon has prismatic peds, large slickensides; red, yellow, and green-grey mottles	F-2a	I-1
P-5. Alfisol	A, AB, Bt	A—Red (2.5YR 5/6, 10R 6/4, 5/6); mottle colours of green-grey (Gley 1 7/10Y) reduction haloes; AB—Red brown (2.5YR 4/4); mottle colours of green-grey (Gley 1 7/10GY) reduction haloes; Bt—Red (10R 4/6, 5/6) and red brown (2.5YR 3/3); mottle colours of green-grey (Gley 1 7/10Y) reduction haloes	A horizon has angular blocky and granular peds; Bt horizon has angular blocky, wedge, and granular peds, clay accumulation, and slickensides; green-grey reduction haloes	F-2a, F-2b	I-1, I-3, I-4, I-5
P-6. Calcic alfisol	A, Bt, Btk	A—Red (10R 5/4), pale red (10R 6/3), and red brown (7.5YR 5/2); mottle colours of red (10R 5/6), grey (10YR 7/2), and green-grey (Gley 1 7/10GY) reduction haloes; Bt—Red (2.5YR 5/6); mottle colours of red-brown (2.5YR 6/4, 7/3) and green-grey (Gley 1 5G8/1) reduction haloes; Btk—Red (10R 4/4, 5/3, 5/4), pale red (10R 6/3), and red grey (10R 6/1); mottle colours of red (2.5YR 5/6, 10R 5/3), red-brown (2.5YR 7/3), and green-grey (Gley 1 8/10GY) reduction haloes	A horizon has angular blocky peds; Bt horizon has angular blocky peds, clay accumulation; Btk horizon has angular blocky peds, clay accumulation, sparse to numerous Stages 2–3 calcium carbonate nodules, rare slickensides; green-grey reduction haloes	F-2a, F-2b	I-1, I-3, I-5, I-9

Table 5

Chinle Formation facies associations.

Facies association	Lithofacies	Ichnocoenoses	Palaeosols	Other features	Palaeoenvironment
FA-1	F-2a, F-3, F-4b, F-4c, F-5a, F-5b	I-5	P-1	Prevalence of coarse-grained lithofacies and trough-cross-stratification; sand bodies form interconnected, stacked, laterally extensive sand sheets; contain wood fragments and log casts; basal erosive contact	Braided river
FA-2	F-5c	N/A	N/A	Incline-bedded conglomerates; ribbon and thin sand sheet bodies surrounded by mudstones and siltstones; large oncoids as clasts	Meandering river
FA-3	F-2a, F-2c, F-3, F-4a, F-5b	I-1, I-2, I-4, I-6, I-7	P-1	Interbedded ripple-cross-laminated sandstone and siltstone; thin, laterally discontinuous sand sheet and ribbon sand bodies; basal erosive contact	Crevasse splay and levee
FA-4	F-1, F-2a, F-2b, F-2c, F-3, F-4a	I-1, I-3, I-5, I-9	P-1, P-2, P-3, P-4, P-5, P-6	Predominance of fine-grained lithofacies; high variety of ichnofossils; well-developed palaeosols	Overbank and floodplain
FA-5	F-1, F-2a, F-2c	I-1, I-2, I-5, I-8	P-1, P-2	Planar-laminated siltstone and very fine-grained sandstone; disruption of bedding by tetrapod tracks and rhizoliths; shallow, horizontal burrows along bedding planes; *Neocalamites*	Palustrine
FA-6	F-2a, F-2c	N/A	N/A	Planar-laminated siltstone and very fine-grained sandstone; rare ichnofossils; desiccation cracks	Lacustrine

is up to 1.3-m deep and 1.45-m long in ripple-cross-laminated sandstone. *Skolithos* is also associated with *Camborygma* in F-3.

Naktodemasis-Camborygma **entisol (IPF IV):** Stacked red, compound AC horizons with the *Naktodemasis-Camborygma* ichnocoenosis (Tables 3–5 Fig. 6D–G) in ripple-cross-laminated very fine sandstone (F-3) within crevasse-splay and levee deposits (FA-3). *Camborygma* is 20–45-cm deep and 25–55-cm long. *Naktodemasis* is 2–5 mm in diameter, overprints the *Camborygma* fill, and penetrates the sediment within beds and between beds. *Scoyenia* are 3–5.5 mm in diameter and are restricted to bedding planes. Green-grey rhizohaloes extend along bedding planes, are 5–20-cm deep, and 6–25-cm long. Only this ichnopedofacies contains occurrences of *Arenicolites*, *Ancorichnus*, and *Treptichnus*.

Rhizolith inceptisol (IPF V): Compound A and AC profiles and the rhizolith ichnocoenosis (Tables 3–5; Fig. 7A–C) in red and red-brown, massive siltstone to very fine sandstone (F-2b) within floodplain deposits (FA-4). Red-brown rhizoliths are up to 16.5-cm deep and 17.5-cm long. Green-grey rhizohaloes are up to 25-cm deep and 26-cm long.

Naktodemasis **inceptisol and calcic inceptisol (IPF VI):** Composite and cumulative A, AB, and ABk horizons and

the *Naktodemasis* ichnocoenosis (Tables 3–5; Fig. 7D–G) in red and red-brown, massive siltstone to very fine sandstone (F-2b) within floodplain deposits (FA-4). Calcic horizons reach mature stage 1 to incipient stage 2 development with sparse calcium carbonate nodules. Green-grey rhizohaloes are 20–95-cm deep, up to 110-cm long, and penetrate underlying horizons. *Naktodemasis* is 2–5 mm in diameter, is found extensively in the entire profile, and overprints rhizohaloes.

Camborygma **inceptisol and calcic inceptisol (IPF VII):** Composite Bk horizons and the *Camborygma* ichnocoenosis (Tables 3–5; Fig. 8A–C) in red and pale red, massive siltstone, and very fine sandstone (F-2b) in floodplain deposits (FA-4). Calcium carbonate nodules have mature stage 2 development. *Camborygma* is 110–120-cm deep and 150-cm long. Green-grey rhizoliths and rhizohaloes are 60-cm deep and 70-cm long.

Therapsid inceptisol and calcic inceptisol (IPF VIII): Composite ABk horizons and the therapsid ichnocoenosis (Tables 3–5; Fig. 8D–F) in red, red-brown, and grey, massive siltstone (F-2a) within floodplain deposits (FA-4). Siltstone is cemented by calcium carbonate and reaches stage 1 development. Therapsid burrows are 175-cm deep, 215-cm long, and overprint multiple ABk horizons. White and yellow rhizoliths are up to 50-cm deep and 80-cm long.
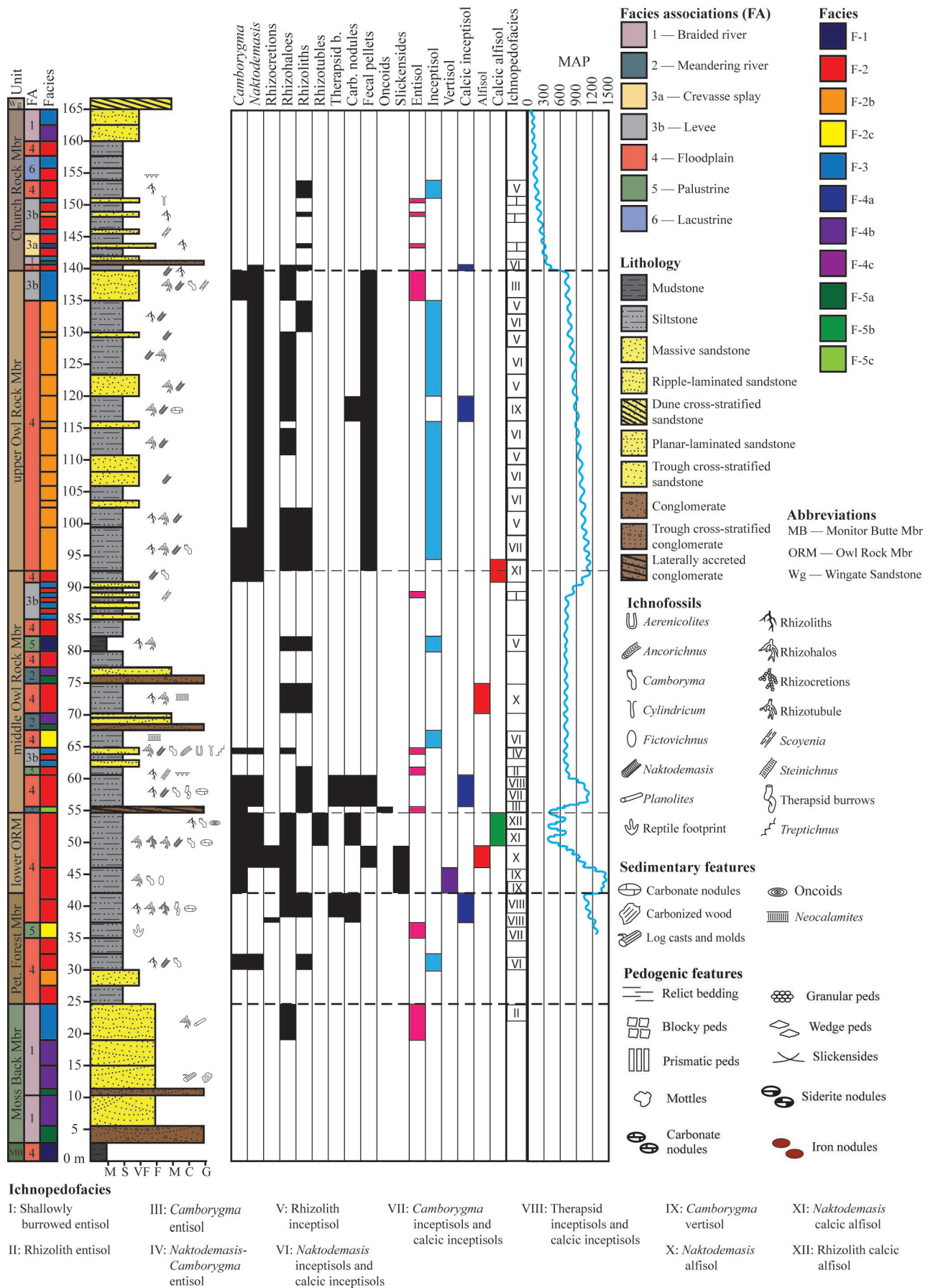
Fig. 4. Distribution of lithofacies, facies associations, ichnofossils, pedogenic features, palaeosols and ichnopedofacies in the Chinle Fm with estimated mean annual precipitation (MAP). Overall, precipitation decreases through time with shorter term wet-dry cyclicity observed in the PFM, lower ORM, and middle ORM.
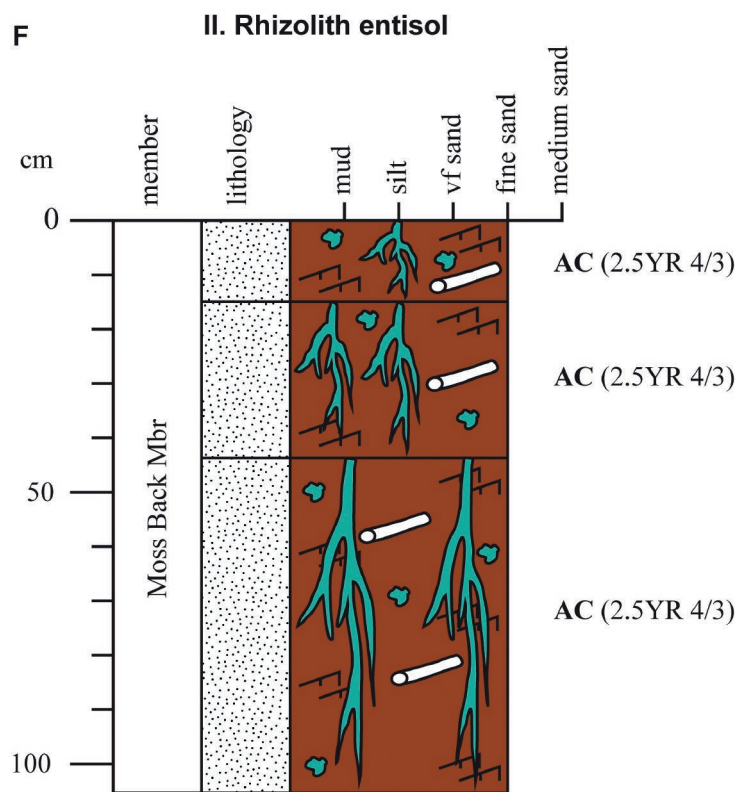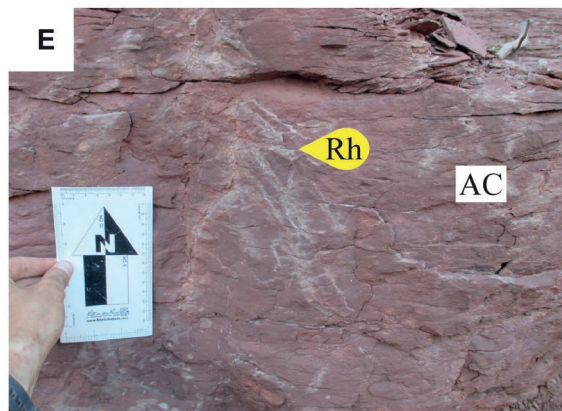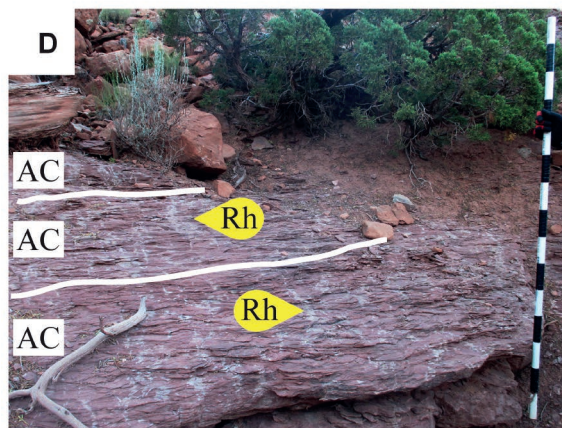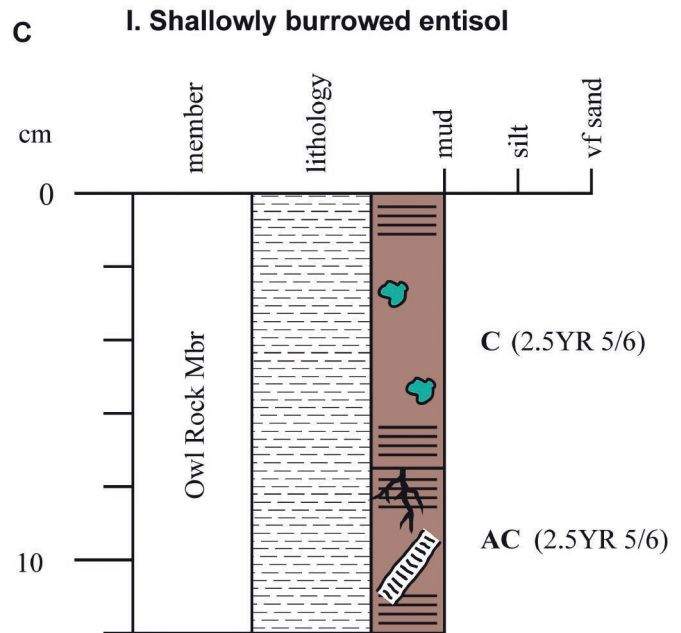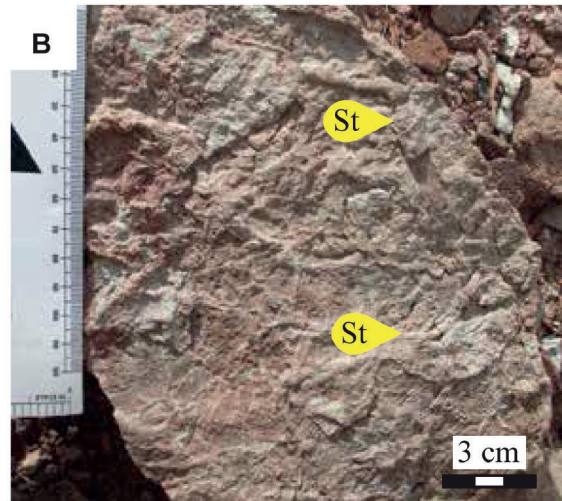
Fig. 5. Diagnostic features of ichnopedofacies I and II. **A.** Stacked AC and C horizons in shallowly burrowed entisol (IPF I). **B.** *Stein-ichnus* (St) covering bottom of bedding planes in IPF I. **C.** Measured section in IPF I. **D.** AC horizons in outcrop with rhizohaloes (Rh) in rhizolith Entisol (IPF II). Staff in 10-cm intervals. **E.** Rhizohaloes (Rh) in the basal AC horizon. Grain size card 15 cm tall. **F.** Measured section in IPF II
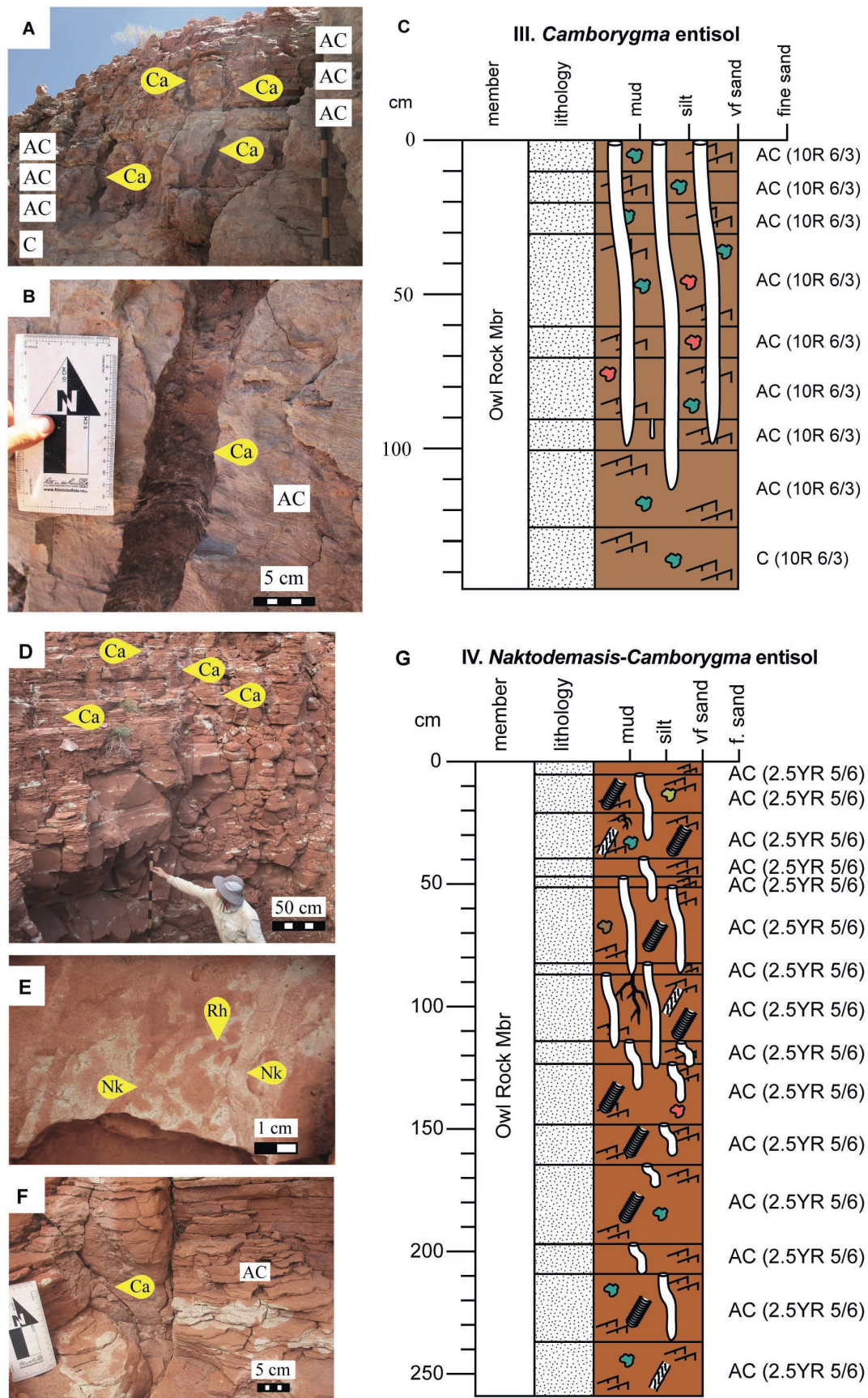
Fig. 6. Diagnostic features of ichnopedofacies III and IV. **A.** 1.1-m-deep *Camborygma* (Ca) penetrating stacked AC horizons in *Camborygma* entisol (IPF III). Staff in 10-cm intervals. **B.** Close-up of *Camborygma* (Ca) in IPF III. Note ripple-lamination preserved around burrow in IPF III. **C.** Measured section in IPF III. **D.** *Camborygma* (Ca) penetrating stacked AC horizons of ripple cross-laminated very fine-grained sandstone in *Naktodemasis-Camborygma* entisol (IPF IV). **E.** *Naktodemasis* (Nk) and rhizoliths (Rh) along bedding planes in IPF IV. **F.** *Camborygma* (Ca) burrow in IPF IV. **G.** Measured section in IPF IV.

Camborygma **vertisol (IPF IX):** Compound to cumulative A-Bss horizons with redoximorphic mottling, slickensides, prismatic peds, and the *Camborygma* ichnocoenosis (Tables 3–5; Fig. 9A–E) in pale red and green-grey, massive siltstone (F-2a) within floodplain deposits (FA-4). *Camborygma* is 75-cm deep, 95-cm long, and extend into the Bss horizon. Rhizohaloes are bright yellow, 60-cm deep, and 70-cm long. *Fictovichnus* is observed 25 cm below the top of the Bss horizon.

Naktodemasis **alfisol (IPF X):** Composite Bt horizons and the *Naktodemasis* ichnocoenosis (Tables 3–5; Fig. 9F–I) in red and red-brown mudstone to siltstone (F-1, F-2a) in floodplain deposits (FA-4). Ichnofossils are only discernible in the A horizon. *Naktodemasis* are 2–5 mm in diameter and green-grey rhizohaloes are 10-cm deep and 12-cm long.

Naktodemasis **calcic alfisol (IPF XI):** Composite Btk horizons and the *Naktodemasis* ichnocoenosis (Tables 3–5; Fig. 10A, B) in red, red-brown, and red-grey, massive siltstone (F-2a) within floodplain deposits (FA-4). Calcium carbonate horizons reach mature stage 2 development. *Naktodemasis* is 2–5 mm in diameter and pentrates down into the Bt horizon. Green-grey rhizohaloes are 19-cm deep and 22-cm long. *Planolites* is <2 mm in diameter and only observed within the A horizon.

Rhizolith calcic alfisol (IPF XII): Composite Btk horizons and the rhizolith ichnocoenosis (Tables 3–5; Fig. 10C–F) in red and red-brown, massive siltstone (F-2a) within floodplain deposits (FA-4). Calcium carbonate accumulation reaches stage 3 development with abundant nodules up to 2 cm in diameter. Rhizotubules lined with calcium carbonate nodules are 120-cm deep and 135-cm long. Green-grey siltstone fills the inside of rhizotubules.

INTERPRETATION OF ICHNOPEDOFACIES

Shallowly burrowed entisol (IPF I): *Cylindricum* in conjunction with F-2c and F-3 suggest subaerially exposed levee, crevasse-splay, and point bar environments with shallow water tables (Figs 5A–C, 11) (Hasiotis and Dubiel, 1993a; Hasiotis and Demko, 1996; Hasiotis, 2004, 2008). This is further supported by the association with desiccation cracks, indicating wetting and drying cycles. *Scoyenia* indicates shallow water tables with sediment saturation near 100% and where the capillary fringe is close to the surface in either marginal-lacustrine or levee environments (Frey *et al.*, 1984; Hasiotis and Dubiel, 1993a; Hasiotis, 2002, 2004, 2008). The occurrence of *Scoyenia* in F-3 suggests deposition on levees or fluvial floodplain. The occurrence of both *Cylindricum* and *Scoyenia* within the same beds (Table 3) indicate fluctuating water-table conditions in these proximal fluvial environments. *Scoyenia* form after initial deposition when water tables and sediment moisture levels are high, then *Cylindricum* is constructed in the deposits as the water table lowers (Hasiotis and Bown, 1992; Hasiotis, 2004, 2008). *Skolithos* are not indicative of any specific environment (Hasiotis, 2002), but the sandstone lenses containing these ichnofossils match the morphology of crevasse-splay deposits (Miall, 1996). *Steinichnus* are associated with palustrine and channel–levee environments with high water tables at or near the sediment-water-air interface (Bromley and Asgaard, 1979; Hasiotis and Bown, 1992; Hasiotis, 2002). Occurrence of *Steinichnus* in green-grey mudstone also supports poorly drained, reducing conditions (Therrien and Fastovsky, 2000; Kraus and Hasiotis, 2006; Smith *et al.*, 2008b). Desiccation cracks and shallow rhizoliths within these mudstones indicate periods of slightly lower water tables and subaerial exposure (Hasiotis *et al.*, 2007a). The close proximity of environments to fluvial systems led to more frequent sedimentation and areas with standing water (swamps, lakes), resulting in shorter duration of pedogenesis between depositional events (Bown and Kraus, 1987, 1993a, b; Kraus, 1999; Hasiotis, 2007; Hasiotis *et al.*, 2012).

Rhizolith entisol (IPF II): Rhizoliths and rhizohaloes in F-4a and F-5b suggest crevasse-splay deposits with high water tables near the sediment surface, restricting vertical penetration by roots (Figs 5D–F, 11) (Hasiotis, 2007; Hasiotis and Platt, 2012). Red-brown rhizoliths within drab green-grey matrix indicate poorly drained sediment (Kraus and Hasiotis, 2006). Green-grey rhizohaloes within red sediment, however, formed by surface water gleying mobilizing and transporting iron oxides away from the original root in well-drained soils (Kraus and Hasiotis, 2006; Smith *et al.*, 2008b). Colour differences in palaeosol matrix, rhizoliths, and rhizohaloes suggest alternating well- and poorly drained conditions after overbank deposition.

Deep penetration of roots in fluvial bars suggests that they became subaerially exposed via falling water level to produce well-drained conditions (Hasiotis *et al.*, 2007a; Counts and Hasiotis, 2014). Fluvial bars were also abandoned during channel migration and became part of the proximal floodplain colonized by plants (Kraus, 1987; Hasiotis, 2004, 2008). Drab colours of rhizohaloes formed through surface water gleying during short periods of standing water during and after flooding events (Retallack, 2001; Hasiotis, 2004, 2008; Kraus and Hasiotis, 2006). Rhizohalo penetration depth decreases upsection from 70 to 15 cm below the sediment surface, indicating a rise in water table through time (Hasiotis, 2004, 2008; Hasiotis *et al.*, 2007a). Weak palaeosol development occurred within close proximity to the fluvial system, indicating frequent flooding and burial by sediment (Bown and Kraus, 1987, 1993a, b; Hasiotis, 2007).

Camborygma **entisol (IPF III):** *Camborygma* extend into the phreatic zone, and mark the level of the palaeowater table (Figs 6A–C, 11) (Hasiotis and Mitchell, 1993; Hasiotis *et al.*, 1993; Hasiotis, 2002). *Camborygma* within F-4a and F-5b are assigned to *Camborygma litonomos* due to their simple shaft morphology and length <0.5 m (Hasiotis and Mitchell, 1993; Hasiotis and Honey, 2000). *Camborygma litonomos* represent saturated sediments with a high-water table in proximal levee, crevasse-splay, and point bar environments (Hasiotis and Mitchell, 1993; Hasiotis *et al.*, 1993; Hasiotis, 2004, 2008). This interpretation is supported by sandstone and conglomerate bodies with morphologies matching proximal fluvial crevasse-splay deposits (Miall, 1996).

Camborygma within F-3 are assigned to *Camborygma eumekenomos* due to shaft depths >1 m and simple mor-
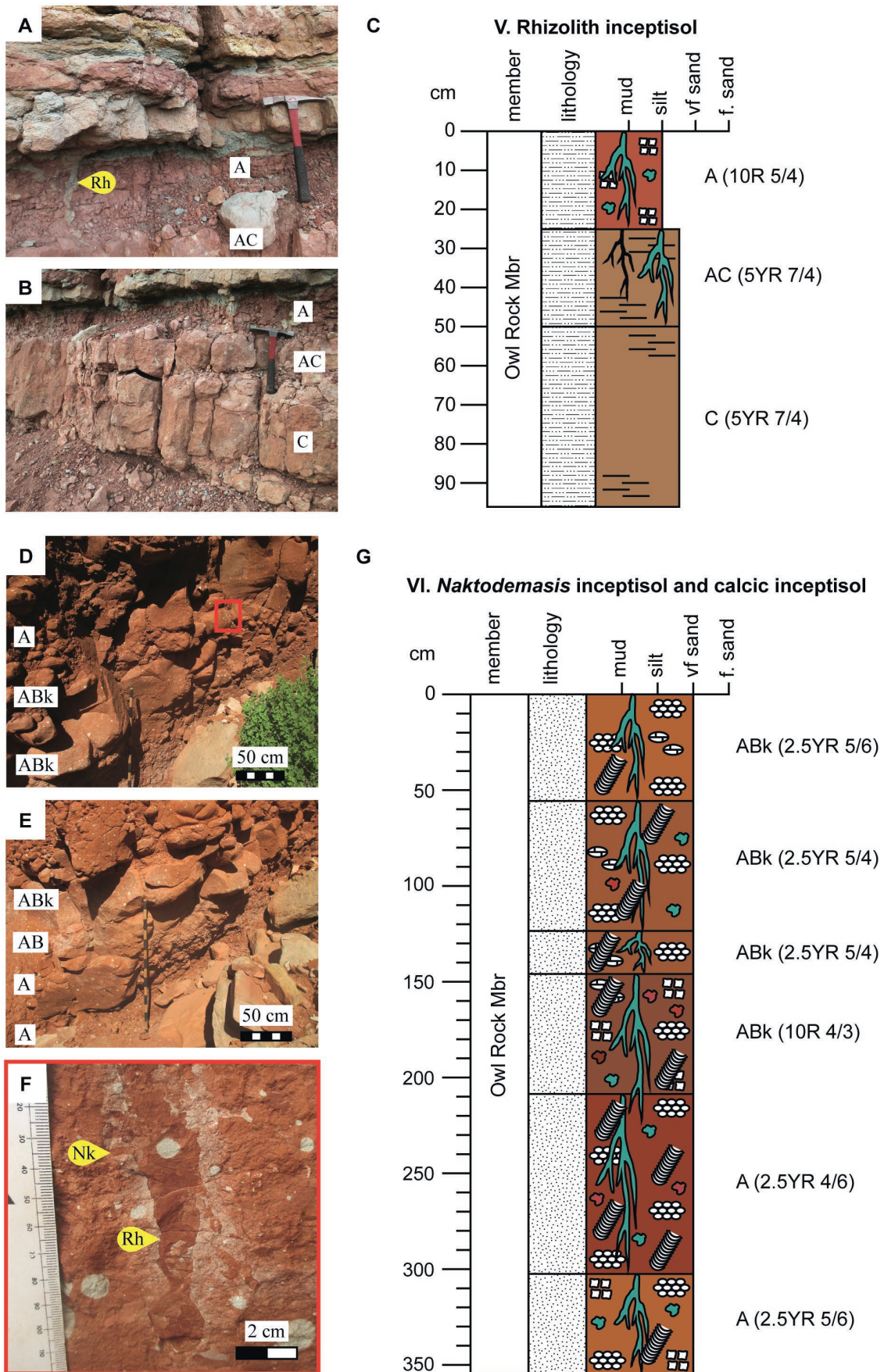
Fig. 7. Diagnostic features of ichnopedofacies V and VI. **A.** Green-grey rhizohalo (Rh) in A horizon in rhizolith inceptisol (IPF V). Rock hammer 33 cm long. **B.** Palaeosol profile in outcrop of IPF V. **C.** Measured section in IPF V. **D, E.** Profile of palaeosol in outcrop of *Naktodemasis* calcic inceptisol (IPF VI). Palaeosols form composite profiles of cumulative horizons in IPF VI. **F.** *Naktodemasis* (Nk) development around a rhizohalo (Rh) in IPF VI. **G.** Measured section in IPF VI.
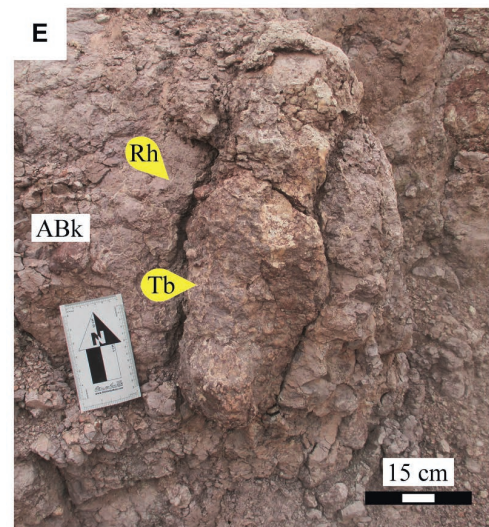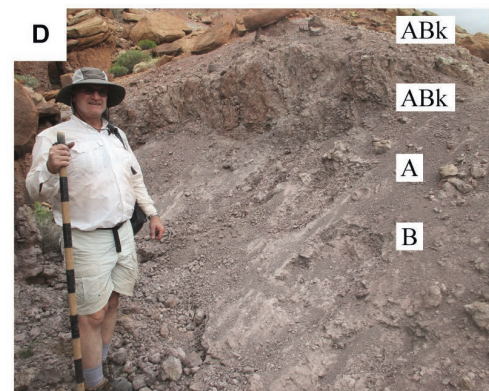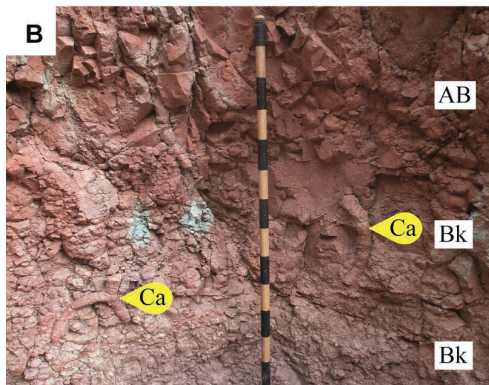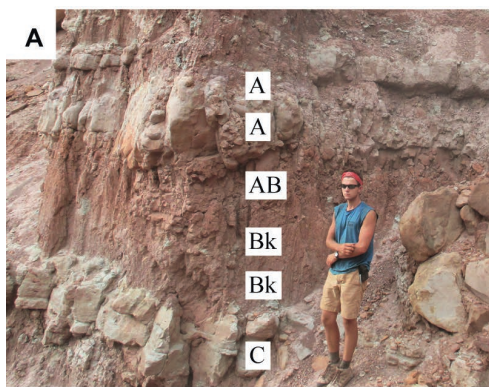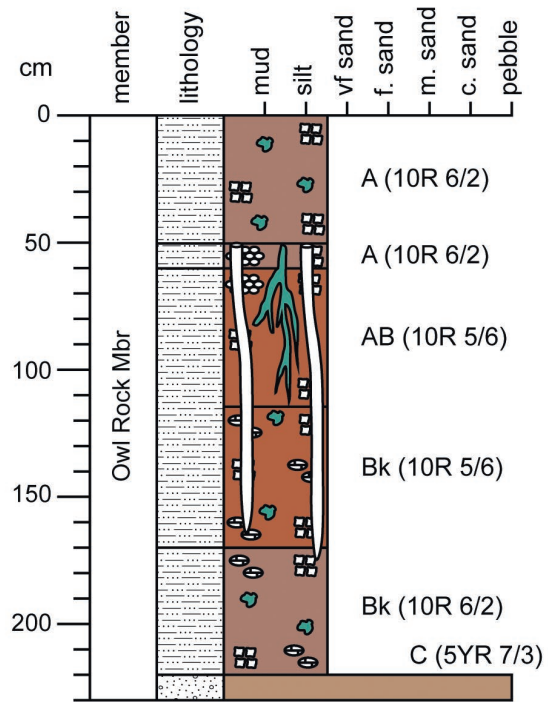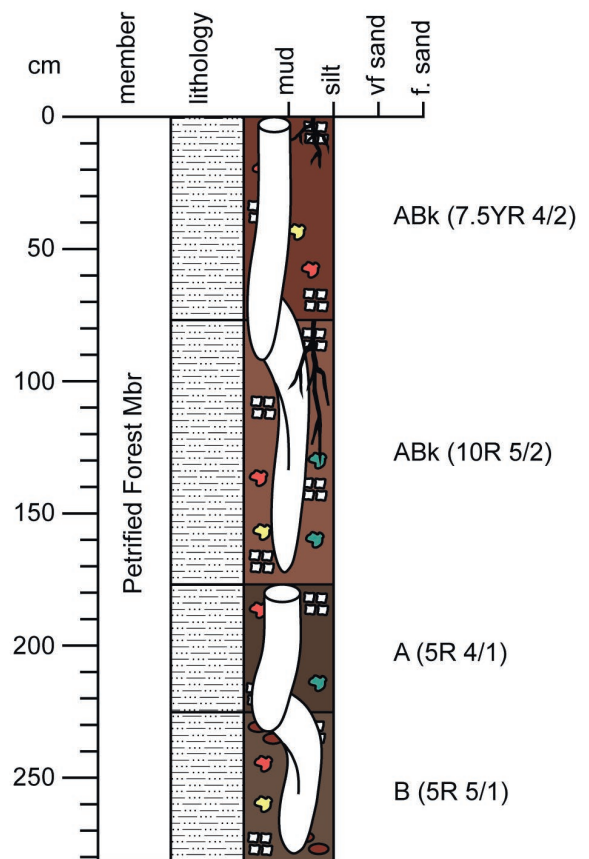
Fig. 8. Diagnostic features of ichnopedofacies VII and VIII. **A.** Palaeosol profile in outcrop of *Camborygma* calcic Inceptisol (IPF VII). Staff in 10-cm intervals. **B.** *Camborygma* (Ca) in branching and nonbranching forms. **C.** Measured section in IPF VII. **D.** Palaeosol profile in outcrop of therapsid calcic inceptisol (IPF VIII). Staff in 10-cm intervals. **E.** Therapsid burrow (Tb) and rhizoliths (Rh) in IPF VIII. **F.** Measured section in IPF VIII.
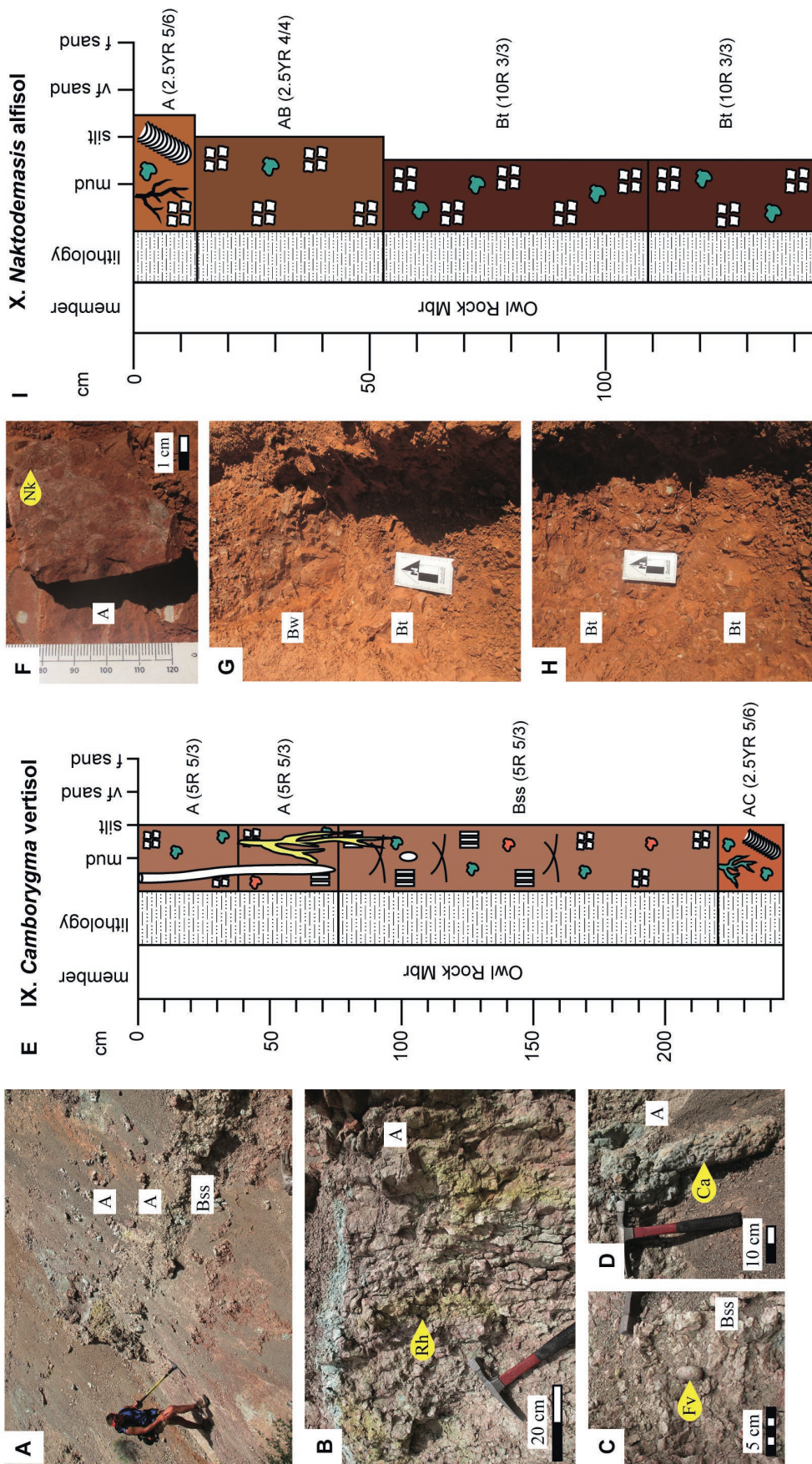
Fig. 9. Diagnostic features of ichnopedofacies IX and X. **A.** Palaeosol profile in outcrop of *Camborygma* vertisol (IPF IX). **B.** Yellow rhizohaloes (Rh) penetrating an A horizon with prismatic peds in IPF IX. **C.** *Fictovichnus* (Fv) in Bss horizon in IPF IX. **D.** *Camborygma* from A horizon in IPF IX. **E.** Measured section in IPF IX. **F.** *Naktodemasis* (Nk) and rhizohaloes in the A horizon in *Naktodemasis* alfisol (IPF X). Grain size card 15 cm tall. **G, H.** Palaeosol profile in outcrop in IPF X. **I.** Measured section in IPF X.
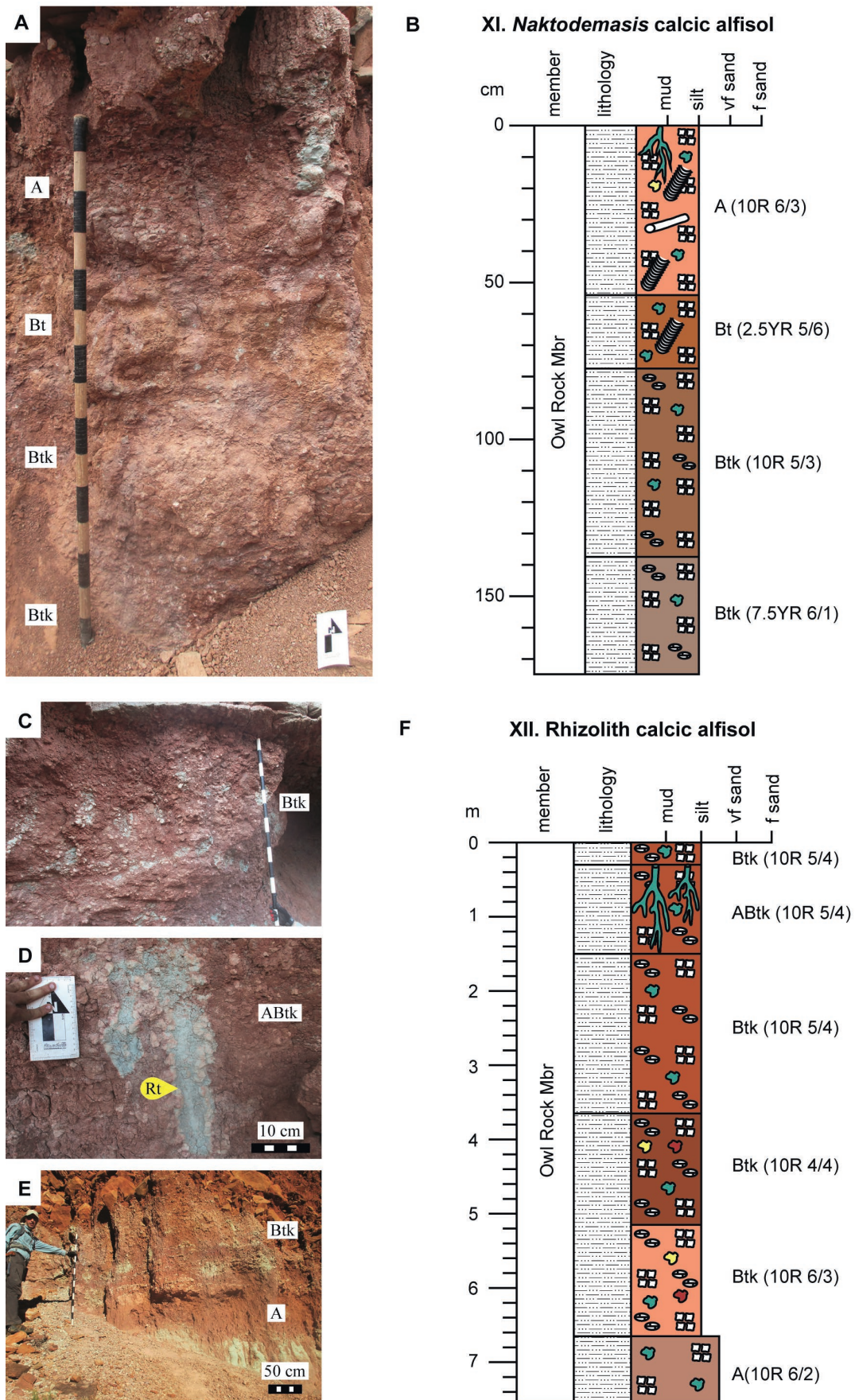
Fig. 10. Diagnostic features of ichnopedofacies XI and XII. **A.** Palaeosol profile in outcrop of *Naktodemasis* calcic alfisol (IPF XI). Staff in 10-cm intervals. **B.** Measured section in IPF XI. **C.** Btk horizon with numerous calcium carbonate nodules in rhizolith calcic alfisol (IPF XII). Top of horizon truncated by overlying conglomerate. Staff in 10-cm intervals. **D.** ABtk horizon with rhizotubules (Rt) lined by calcium carbonate nodules in IPF XII. **E.** Lower half of palaeosol profile in outcrop of IPF XII. Note sharp contrast between $CaCO_3$-bearing Btk horizon and underlying A horizon. **F.** Measured section in IPF XII.

Fig. 11. Ichnopedofacies depositional model for Chinle Fm. Lateral distribution of ichnopedofacies on alluvial plain. Cross-section from A to A' on landscape block diagram shows variations in physiochemical conditions along the alluvial plain. Shallower burrows located closer to fluvial channel, whereas deeper burrows and CaCO$_3$ nodules occur on distal floodplain.

phology (Hasiotis and Mitchell, 1993; Hasiotis et al., 1993). *Camborygma eumekenomos* indicate deeper, highly fluctuating water tables in proximal floodplain environments (Hasiotis and Mitchell, 1993; Hasiotis and Honey, 2000; Hasiotis, 2004, 2008). Stacked compound AC horizons first formed on levees during an interval of nonsteady, high sedimentation (Fig. 6A–C; Kraus, 1999; Hasiotis and Platt, 2012). *Skolithos* formed during short intervals of pedogenesis between depositional episodes, suggesting other bioturbation may have occurred within AC horizons but is not clearly visible. Close proximity to the fluvial system led to frequent burial by sediment, restricting pedogenic development and preserving primary sedimentary structures (Bown and Kraus, 1987; Hasiotis et al.., 2012). *Camborygma* originated from a stable soil surface during a hiatus in sedimentation, allowing burrows to overprint the underlying AC horizons (Hasiotis and Honey, 2000). Occurrence of *C. eumekenomos* also marks the migration of the fluvial system away from the area, which led to less frequent sedimentation events and greater pedogenesis (e.g., Bown and Kraus, 1993a, b; Hasiotis, 2004, 2008).

Naktodemasis-Camborygma **entisol (IPF IV):** This ichnopedofacies contains ichnofossils representing both high and low water tables. The occurrence of *Scoyenia, Arenicolites, Ancorichnus*, and *Treptichnus* along bedding planes

suggests a shallow water table and intervals of standing freshwater (Figs 6D–G, 11) (Hasiotis, 2002, 2004, 2008). *Camborygma litonomos* also indicate a shallow water table between 20–45 cm beneath the sediment surface. *Naktodemasis*, however, reflect terraphilic to hygrophilic behaviour and indicates moderate- to well-drained soil conditions (e.g., Hasiotis, 2004, 2008; Smith *et al.*, 2008a, b; Counts and Hasiotis, 2009, 2014). Green-grey rhizohaloes penetrating up to 20 cm deep further support a thin, well-drained vadose zone (Kraus and Hasiotis, 2006; Hasiotis *et al.*, 2007a; Counts and Hasiotis, 2014).

Overprinting of ichnofossils exhibiting terraphilic, hygrophilic, and hydrophilic behaviours are common features in fluvial deposits and indicate fluctuating water tables (Hasiotis and Bown, 1992; Hasiotis, 2002). After initial sediment deposition, when standing water was present, the levee was colonized with *Arenicolites, Ancorichnus*, and *Treptichnus*. As water level fell beneath the sediment surface, *Scoyenia* and shallow roots penetrated the levee. Continued pedogenesis and improved drainage allowed the tracemakers of *C. litonomos* and *Naktodemasis* to bioturbate the sediment and overprint previous burrows. Towards the end of pedogenesis, deeper penetrating roots, in turn fed on by the organisms producing *Naktodemasis,* overprinted *C. litonomos*. Pedogenesis was brief due to close proximity

to the fluvial system that frequently deposited new sediment onto the levee, which subsequently underwent pedogenesis after the water level lowered. This pattern was repeated over time (Bown and Kraus, 1987, 1993a, b; Hasiotis and Bown, 1992; Hasiotis, 2007).

Rhizolith inceptisol (IPF V): Vertically penetrating, green-grey rhizohaloes and red-brown rhizoliths and strong red colour of palaeosols indicate well-drained conditions (Figs 7A–C, 11) (Kraus and Hasiotis, 2006). Root ichnofossils, however, only show a maximum penetration depth of 25 cm, indicating the vadose zone was thin and the water table was shallow (Hasiotis *et al.*, 2007a). The compound profiles indicate high, nonsteady sedimentation with pedogenesis occurring between depositional events (Kraus, 1999; Hasiotis and Platt, 2012). The AC horizon with remnant bedding indicates shorter duration pedogenesis than the overlying homogenized A horizon (Bown and Kraus, 1987; Hasiotis *et al.*, 2012). Incipient horizon formation, nonsteady sedimentation, short duration of pedogenesis, and shallow water tables indicate a proximal position on the floodplain (Bown and Kraus, 1987, 1993a, b; Birkeland, 1999; Hasiotis and Platt, 2012).

***Naktodemasis* inceptisol and calcic inceptisol (IPF VI):** Extensive *Naktodemasis* development, deeply penetrating rhizohaloes, and strong red palaeosol colouration suggest well-drained environments with a deep water table (Figs 7D–G, 11) (Kraus and Aslan, 1993; Kraus and Hasiotis, 2006; Hasiotis *et al.*, 2007a; Smith *et al.,* 2008a; Counts and Hasiotis, 2009, 2014). Calcium carbonate nodules indicate that evapotranspiration > precipitation (Gile *et al.*, 1966; Machette, 1985), and also support the interpretation of well-drained conditions. The length of pedogenesis allowed roots to crosscut underlying horizons and *Naktodemasis* to form around these roots as feeding behaviour (Fig. 7F). Cumulative and composite profiles formed when pedogenesis outpaced steady state and nonsteady state sediment deposition, respectively, leading to more developed palaeosols (Kraus, 1999; Hasiotis and Platt, 2012), and suggesting a more distal position on the floodplain (Bown and Kraus, 1987, 1993a, b; Hasiotis, 2007; Hasiotis *et al.*, 2012).

***Camborygma* inceptisol and calcic inceptisol (IPF VII):** *Camborygma eumekenomos* terminates at a pale red Bk horizon, indicating a deep, highly fluctuating water table at times >1 m below the sediment surface. Pale red colouration is associated with less well-drained palaeosol horizons (Figs 8A–C, 11) (Kraus and Aslan, 1993; Kraus and Hasiotis, 2006; Smith *et al.*, 2008b, c), supporting more frequent saturated conditions at this level. Stronger red colouration in overlying horizons, roots, faecal pellets, and calcium carbonate nodules indicate well-drained, oxidizing conditions higher in the palaeosol profile (Kraus and Aslan, 1993; Kraus and Hasiotis, 2006; Hasiotis and Platt, 2012). Calcium carbonate nodules overprinted *C. eumekenomos* and the pale red Bk horizon during extended intervals of lower precipitation and palaeowater table, suggesting evapotranspiration outpaced precipitation and moisture was highly seasonal (Machette, 1985; Dubiel and Hasiotis, 2011). Composite horizons indicate pedogenesis outpaced nonsteady state sediment deposition on the distal floodplain, leading to better developed palaeosols (Kraus, 1999; Hasiotis and Platt, 2012).

Therapsid inceptisol and calcic inceptisol (IPF VIII): Therapsid burrows exhibit terraphilic behaviour and were constructed above the water table (Figs 8D–F, 11) (Hasiotis, 2004, 2008; Hasiotis *et al.*, 2004, 2007b; Hembree and Hasiotis, 2008). Two episodes of colonization by therapsids are observed. The lower therapsid burrows occur in horizons with duller colour values and iron oxide nodules, which indicate higher moisture, higher sediment saturation, and more poorly drained conditions (Kraus and Aslan, 1993; Mack *et al.*, 1993; Stiles *et al.*, 2001). Therapsid burrows were emplaced during an interval of sediment hiatus and stable landscape with well-drained conditions of relatively short duration. The upper two ABk horizons denote two intervals of sedimentation and subsequent bioturbation by roots and invertebrates. Deep rhizoliths and stronger red colouration indicate well-drained palaeosols with longer pedogenesis, allowing therapsid burrows to overprint horizons and carbonate to the buildup in the profile. Composite calcic horizons indicate pedogenesis outpaced sediment deposition in a distal position on the floodplain (Bown and Kraus, 1993a, b; Kraus, 1999; Hasiotis *et al.*, 2007a; Hasiotis and Platt, 2012).

***Camborygma* vertisol (IPF IX):** Redoximorphic colouration, prismatic peds, and slickensides indicate fluctuating water tables and seasonal moisture (Figs 9A–E, 11) (Driese and Foreman, 1992; Driese and Mora, 1993; Kraus and Hasiotis, 2006; Dubiel and Hasiotis, 2011). *Fictovichnus* are cocoons that represent terraphilic behaviour in well-drained sediments constructed during the dry season when soil moisture and the water table were lower (Hasiotis, 2002, 2003, 2004, 2008). Subsequent water table rise during the wet season aided in preservation of the cocoons (Alonso-Zara *et al.*, 2014). Following an interval of deposition, plants colonized the soil profile and yellow rhizohaloes formed in saturated, poorly drained sediments with reducing conditions (Kraus and Hasiotis, 2006). Another interval of deposition followed, and a subsequent hiatus in sedimentation allowed for *C. eumekenomos* to overprint underlying horizons to a water table depth ~75 cm below the sediment surface. The redoximorphic colouration, compound and cumulative profiles, and *C. eumekenomos* indicate a proximal position on the floodplain (Kraus, 1987; Hasiotis and Mitchell, 1993; Kraus, 1999; Hasiotis and Platt, 2012).

***Naktodemasis* alfisol (IPF X):** *Naktodemasis* as feeding behaviour around roots and red matrix indicates well-drained conditions with a low water table (Figs 9F–I, 11) (Kraus and Aslan, 1993; Kraus and Hasiotis, 2006; Smith and Hasiotis, 2008; Smith *et al.*, 2008a; Counts and Hasiotis, 2009, 2014). Composite Bt horizons formed as pedogenesis outpaced sedimentation, allowing clay to accumulate in the subsurface, indicating a more stable landscape in a distal position on the floodplain (Bown and Kraus, 1987; Kraus, 1999; Hasiotis *et al.*, 2007a; Hasiotis and Platt, 2012).

***Naktodemasis* calcic alfisol (IPF XI):** *Naktodemasis* developement down 75 cm, calcium carbonate nodules, and red colouration indicate well-drained conditions with a deep water table produced when evapotranspira-

tion outpaced precipitation and moisture was seasonal (Figs 10A, B, 11) (Machette, 1985; Counts and Hasiotis, 2014). Composite Btk profiles indicate that pedogenesis outpaced sedimentation, allowing clay accumulation and carbonate buildup in a landscape on the distal floodplain (Bown and Kraus, 1993a, b; Kraus, 1999; Hasiotis, 2007; Hasiotis and Platt, 2012).

Rhizolith calcic alfisol (IPF XII): Red matrix, deeply penetrating rhizotubules, and carbonate nodules indicate well-drained conditions with a deep water table when evapotranspiration outpaced precipitation and moisture was seasonal. Rhizotubules formed as carbonate precipitated on root surfaces during the uptake of nutrients and water (Figs 10C–F, 11) (Klappa, 1980; Kraus and Hasiotis, 2006), which produced a cylinder that conducted water in the soil profile (Klappa, 1980), producing a gleyed matrix (reducing conditions) within the rhizotubule. The Btk horizon above the rooted zone indicates another calcic alfisol formed on top of this profile, but was cut out by the overlying conglomerate. Abundant accumulation of carbonate and well-formed, composite Btk horizons indicate greater duration of palaeosol development with pedogenesis outpacing sedimentation on the most distal position of the floodplain.

DISTRIBUTION OF PALAEOSOLS AND ICHNOPEDOFACIES

Lateral distribution

Ichnopedofacies show an inverse relationship between palaeosol development and proximity to the fluvial system in a general model (Fig. 11). Entisol ichnopedofacies (IPF-I–IV) are restricted to proximal fluvial bar, crevasse-splay, and levee environments. Inceptisol, calcic inceptisol, vertisol, alfisol, and calcic alfisol ichnopedofacies (IP-V–XII) are only present in floodplain environments. This distribution shows a similar pattern to palaeosols of the Palaeogene Willwood Fm in Wyoming, where Bown and Kraus (1987, 1993a, b) and Kraus (1987) attributed their observations of palaeosol development to decreasing short-term sediment accumulation rates with increasing distance from the channel. Thinning of fluvial deposits away from the channel means distal environments experience less sedimentation and greater duration of pedogenesis (Bown and Kraus, 1987, 1993a, b; Hasiotis, 2002, 2007). Rhizolith inceptisols show greater development than other ichnopedofacies in channel bank, crevasse-splay, and levee environments, but pedogenesis did not act long enough for the development of calcic or argillic horizons, indicating formation on the proximal floodplain. The strong hydromorphic features of *Camborygma* vertisols indicate areas of low topography on the floodplain, leading to higher gleyed matrixes and less well-drained conditions (Kraus and Middleton, 1987a; Kraus and Aslan, 1993; Prochnow *et al.*, 2005). Lack of carbonate accumulation further supports higher moisture content in this ichnopedofacies. *Naktodemasis* inceptisols and calcic inceptisols, *Camborygma* inceptisols and calcic inceptisols, and therapsid inceptisols and calcic inceptisols display more developed horizonation, supporting formation

on the distal floodplain. *Naktodemasis* alfisols, *Naktodemasis* calcic alfisols, and rhizolith calcic alfisols show both thick, well-developed calcic and argillic horizons, also indicating a distal floodplain position.

Vertical distribution

Overall, ichnofossil diversity increases from the MM into the lower and middle ORM, then decreases throughout the rest of the ORM and CRM. Calcium carbonate nodules are most abundant in the PFM, lower ORM, and base of the middle ORM and decrease in occurrence up section (Figs 4, 12). Ichnopedofacies tend to redden up section and become dominated by ichnofossils displaying terraphilic behaviour. *Camborygma* decrease in occurrence through ORM deposition and are absent from the CRM. Therapsid burrows, conspicuous in the PFM, decrease up section through the ORM and are absent from the CRM. Root ichnofossils and *Naktodemasis* occur throughout the PFM and ORM, though *Naktodemasis* are only present near the base of the CRM, whereas root ichnofossils persist higher into this unit. Rhizoliths and *Cylindricum* are the stratigraphically highest occurring ichnofossils in the Chinle Fm.

Proximal fluvial (i.e., channel, levee, crevasse splay) deposits show a stratigraphic shift in ichnopedofacies throughout the Chinle Fm (Fig. 4). Rhizolith entisols in the MM transition to *Camborygma* entisols in the PFM. *Camborygma* entisols transition to both shallowly burrowed entisols, dominated by the *Steinichnus* and *Scoyenia* ichnocoenoses, and *Camborygma-Naktodemasis* entisols in the ORM. Ichnopedofacies transition to shallowly burrowed entisols, dominated by the *Scoyenia* and *Cylindricum* ichnocoenoses, and rhizolith entisols in the CRM.

Proximal and distal floodplain deposits also display stratigraphic changes in ichnopedofacies (Figs 4, 12). Floodplain ichnopedofacies are rare in the MM, but the PFM contains *Naktodemasis* inceptisols and calcic inceptisols, and therapsid inceptisols and calcic inceptisols. These ichnopedofacies transition to *Camborygma* vertisols, rhizolith inceptisols, *Naktodemasis* calcic alfisols, and rhizolith calcic alfisols in the lower ORM. In the middle to upper ORM, ichnopedofacies consist of *Camborygma* inceptisols and calcic inceptisols, *Naktodemasis* alfisols, and *Naktodemasis* inceptisols and calcic inceptisols. Ichnopedofacies transition to *Naktodemasis* inceptisols and calcic inceptisols and rhizolith inceptisols in the CRM.

INCISED VALLEYS AND CHANNEL FILLS

Pedogenic development was further influenced by topographic position and location within the study area. Stacked palaeovalleys are present in all members, and palaeosols fill these palaeovalleys (Fig. 12). Palaeovalley depth varies from 5–17 m, indicating significant variation in palaeotopography during Chinle Fm deposition. In the PFM, lower ORM, and upper ORM, less developed palaeosols dominate palaeovalleys and better developed palaeosols occur on interfluve positions. A position on the interfluve itself, however, is not indicative of a particular stage of palaeosol development. Inceptisols and vertisols were more common
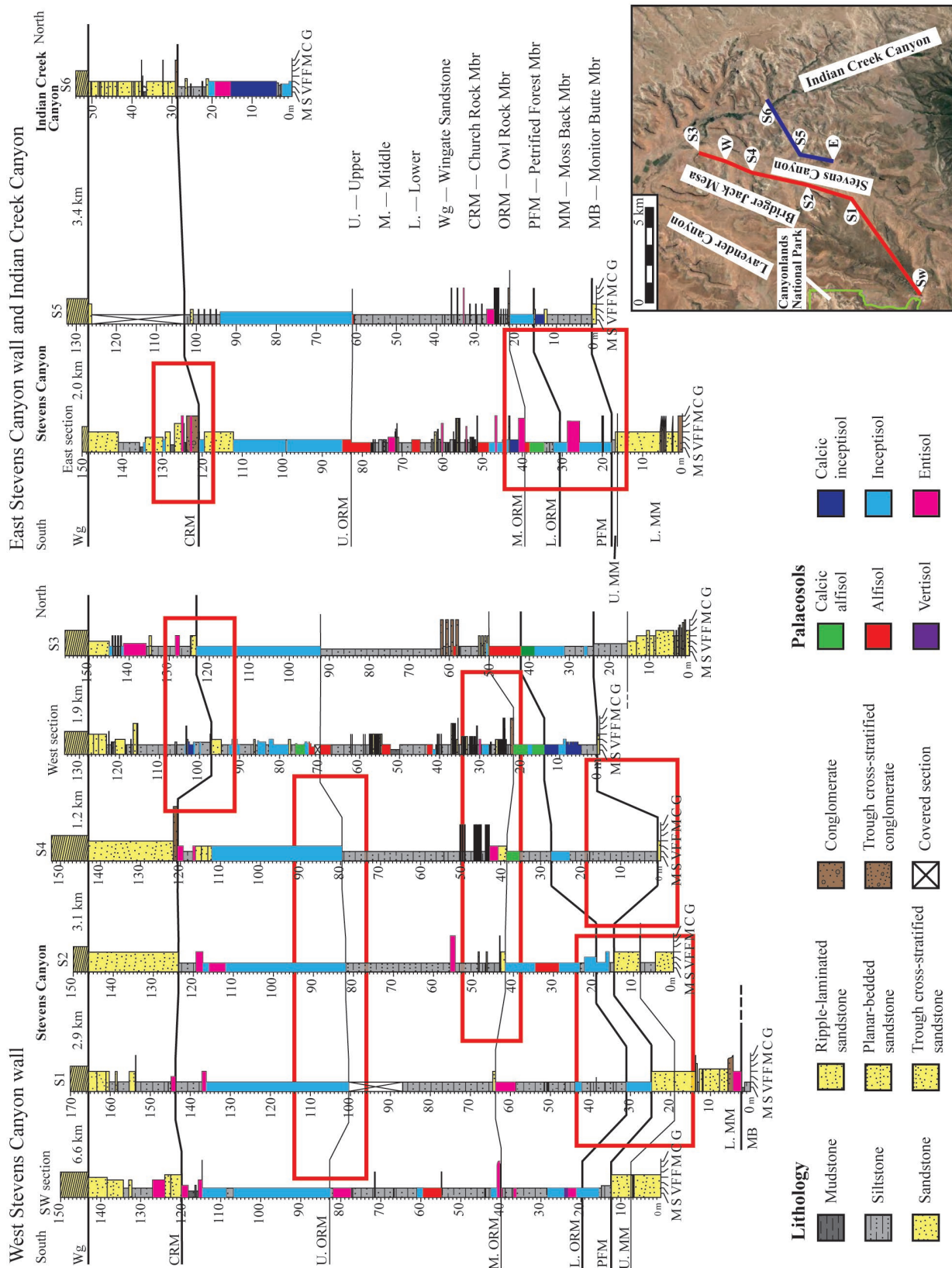
Fig. 12. Correlation panel of the measured stratigraphic sections. Red boxes highlight Chinle Fm palaeovalleys. Palaeovalleys cut into all members during base-level fall and filled during base-level rise.

at interfluve locations in the south of the study area. Calcic inceptisols, alfisols, and calcic alfisols were more common on interfluves located towards the north of the study area. This indicates a local trend from PFM into ORM deposition, where lower valley-fill rates with longer duration of pedogenesis were present in the north, with rate of valley fill increasing to the south. No trend is associated with palaeosol development and topographic position for palaeovalleys in the MM, middle ORM, and CRM.

PHYSIOCHEMICAL CONTROLS ON SEDIMENTATION AND ICHNOPEDOLOGIC DEVELOPMENT IN THE NORTH-EASTERN CHINLE BASIN

Physiochemical conditions controlling sedimentation and ichnopedofacies development in the north-east Chinle Basin can be separated into autocyclic controls, allocyclic controls, and hydrology. Autocyclic processes are determined by energy distribution within the depositional basin and include fluvial channel migration and overbank flooding events (Beerbower, 1964; Allen, 1970; Bridge and Leeder, 1979; Bridge, 1984; Smith *et al.*, 1989; Slingerland and Smith, 2004; Cleveland *et al.*, 2007; Trendell *et al.*, 2012). Allocyclic controls are influences from outside of the depositional basin and include tectonism (including halokinesis) and climate (Beerbower, 1964; Cater, 1970; Bridge and Leeder, 1979; Blakey and Gubitosa, 1983; Alexander and Leeder, 1987; Hazel, 1994; Cecil, 2003; Cleveland *et al.*, 2007; Dubiel and Hasiotis, 2011). Hydrology is influenced by autocyclic and allocyclic processes and controls the distribution, tiering, and depth of ichnofossils (Hasiotis and Bown, 1992; Hasiotis and Mitchell, 1993; Hasiotis and Dubiel, 1994; Hasiotis, 2002, 2004, 2007, 2008; Hasiotis *et al.*, 2007a, 2012).

Autocyclic processes

Within the Chinle Fm, meandering river, braided river, crevasse-splay, and levee deposits commonly overlie floodplain deposits (Fig. 4). This depositional pattern records overbank flooding and channel migration on the alluvial plain, with pedogenesis occurring between depositional events (Bridge and Leeder, 1979; Bridge, 1984; Kraus, 1987, 1999, 2002; Smith *et al.*, 1989; Slingerland and Smith, 2004).

Overbank flooding: This depositional process is preserved in the PFM, middle ORM, and CRM where the thin, discontinuous nature of sandstone facies indicates deposition on the distal ends of prograding crevasse-splay and levee complexes (Bridge, 1984; Bown and Kraus, 1987). Frequency of overbank flooding influenced up section changes in palaeosol development. Alfisols occur between depositional episodes in the PFM and middle ORM (Fig. 12). Alfisols decrease up section and no alfisols are found within the CRM (Figs 4, 12). Alfisols in the PFM and middle ORM indicates these units had longer durations of pedogenesis between depositional events. The frequency and magnitude of sedimentation by overbank flooding increased in the CRM (Bown and Kraus, 1993a,

b; Hasiotis, 2007; Hasiotis *et al.*, 2007a), which reduced the duration of pedogenesis and resulted in a transition from the formation of calcic inceptisols to the formation of inceptisols and entisols.

Channel migration: This depositional process is preserved in the MM, PFM, ORM, and CRM where channel migration of braided and meandering rivers influenced sediment deposition and duration of pedogenesis (Figs 4, 12). Channel migration towards distal positions on the floodplain led to more frequent sedimentation events and laid levee and crevasse-splay deposits over floodplain deposits, interrupting pedogenesis. Subsequent fluvial migration away from the area resulted in less frequent sedimentation and greater duration of pedogenesis, allowing crevasse-splay and levee deposits to be topped by more developed ichnopedofacies (Kraus, 1987; Bown and Kraus, 1993a, b; Hasiotis *et al.*, 2007a).

Frequency of channel migration changed through Chine Fm deposition, affecting the development of palaeosols and ichnopedofacies. In the MM, frequent migration of braided rivers led to the abandonment of fluvial bars and the development of rhizolith entisols on bar tops. Channel migration frequency then decreased during deposition of the PFM and lower ORM. Decreased reworking by meandering fluvial systems with low, nonsteady sedimentation allowed for greater duration of pedogenesis. Numerous channel migration deposits in the middle ORM indicate an increase in migration frequency up section. Frequency of channel migration then decreased during upper ORM deposition, with only one channel migration event observed near the top of the unit. Less frequent channel migration, and a shift to relatively steady sediment deposition allowed for the accumulation of composite and cumulative palaeosol profiles. Channel migration frequency then increased once again during CRM deposition. Increased channel migration and increasing nonsteady sediment deposition led to shorter duration of pedogenesis and a transition from composite inceptisols to compound inceptisols and entisols.

Comparison to FACs: In the north-east Chinle Basin, overbank flooding and channel migration deposits fine upward similarly to the meter-scale fluvial aggradational cycles (FACs) observed in the Chinle Fm in Arizona, New Mexico, and eastern Utah (Prochnow *et al.*, 2006b; Cleveland *et al.*, 2007; Trendell *et al.*, 2012). In the study area, however, such nested fluvial cycles were not identified; though channel migration and overbank flooding did affect finer scale sedimentation patterns. The absence of nested fluvial cyclicity indicates that autocyclic processes were neither as common nor the dominant control on sedimentation.

Allocyclic processes

Regional tectonism: Changes in rates of basin subsidence and accommodation are indicated by shifting styles of fluvial deposition and ichnopedofacies development (Figs 4, 12). Low subsidence rates led to decreased accommodation, causing increased reworking of sediment by fluvial systems (e.g., Kraus and Middleton, 1987b). Frequent reworking of sediment resulted in poor preservation of ichnopedofacies in the MM, and those that were preserved were less developed due to short duration of pedogenesis. Fluvial styles

evolved into meandering streams in the PFM and ORM. The thick floodplain deposits and ribbon sand bodies of these units support rapid subsidence rates that allowed for greater accommodation in the basin (Blakey and Gubitosa, 1984; Kraus, 1987; Kraus and Middleton, 1987b; Hazel, 1994; Cleveland *et al.*, 2007). Greater accommodation meant less frequent sediment reworking by rivers and longer duration of pedogenesis (Bown and Kraus, 1987; Blakey and Gubitosa, 1984; Kraus, 2002). This aided in the formation and preservation of more developed ichnopedofacies in the PFM and lower ORM. During intervals of higher sedimentation, floodplain and fluvial systems aggraded (e.g., Smith *et al.*, 1989; Slingerland and Smith, 2004). Intervals of higher nonsteady and steady sedimentation explain the formation of compound and composite ichnopedofacies in the middle ORM and composite and cumulative ichnopedofacies in the upper ORM. Sand sheets in the CRM indicate a shift to lower basin subsidence rates at the end of Chinle Fm deposition (Blakey and Gubitosa, 1983, 1984; Kraus, 1987; Hazel, 1994; Cleveland *et al.*, 2007). Ribbon sand bodies in the CRM, however, indicate basin subsidence rate was not as low as during MM deposition. Slightly higher subsidence rates allowed for the accommodation needed for the preservation of playa lake deposits in the CRM. As basin subsidence decreased, accommodation also decreased and sediment reworking by fluvial systems increased. Shorter duration pedogenesis led to less developed ichnopedofacies up section, though frequent cannibalization of sediment by rivers meant some ichnopedofacies were not preserved in CRM deposits.

Incised valleys formed through base-level changes, and ichnopedofacies filling these valleys were influenced by temporal and spatial changes in sedimentation rate. Drops in base level cut valleys into Chinle Fm units and mark the breaks between members. Valleys were subsequently filled during rises in base level, which created accommodation for sedimentation. During MM deposition, high, nonsteady sedimentation rates and increased fluvial migration during reduced accommodation influenced the formation of entisols. During PFM, lower ORM, and upper ORM deposition, relative rates of valley fill were higher in the south of the study area than in the north, creating a trend of increasing duration of pedogenesis on interfluves located to the north. Overall sedimentation rates remained fairly low during PRM and lower ORM deposition. Low, nonsteady sedimentation, along with rare channel migration, further enhanced the formation of well-developed ichnopedofacies including compound and composite inceptisols and alfisols. Sedimentation rates then increased and remained predominantly nonsteady during middle ORM deposition. Sedimentation remained high, but decreased slightly and become relatively steady in the upper ORM. Sedimentation rates increased in the CRM and also shifted to nonsteady deposition. This change in sedimentation, in conjunction with decreased basin accommodation and more frequent channel migration, resulted in a shift from inceptisols at the base of the member to poorly developed, compound entisols and inceptisols.

Halokinesis: This process influenced facies distribution and preservation in the study area. The north-east Chinle Basin is located at the western edge of the Salt Anticline Region, and previous investigations have noted that halokinesis influenced sedimentary architecture and palaeosol development (Blakey and Gubitosa, 1983; Hazel, 1994; Prochnow *et al.*, 2005, 2006b). Across the Four Corners region, including south-eastern Utah, extensive lacustrine limestone beds have been identified within the ORM (Stewart *et al.*, 1972; Blakey and Gubitosa, 1983; Dubiel, 1987). The ORM in the study area, however, does not contain those extensive lacustrine limestone beds. A laterally accreted conglomerate bed containing oncoid clasts occurs instead in that stratigraphically equivalent position (Figs 4, 12). Increased basin subsidence due to salt withdrawal during lower ORM deposition created the accommodation needed for lakes to form. Oncolites then developed within this local lacustrine system (e.g., Abell *et al.*, 1982; Rosell and Obrador, 1982; Parcerisa *et al.*, 2006; Arenas *et al.*, 2007). Following lake development, a drop in local base level caused by salt diapirism led to fluvial incision and reworking of the lacustrine deposits (Blakey and Gubitosa, 1983, 1984; Hazel, 1994). Oncolites composing the gravel in the lateral accretion beds are the only evidence of the lacustrine system.

Climate: Climatic trends are interpreted from vertical changes of ichnopedofacies, particularly those with pedogenic carbonate. Modern locations in India and Tanzania were selected as the most appropriate analogues to Chinle Fm palaeosols due to their monsoonal conditions with similar environments and latitudinal positions to deposits in the Chinle Fm.

Stage 1 carbonate buildup in PFM ichnopedofacies was primarily influenced by precipitation levels. Modern soils in central India (~20–30°N) under monsoonal conditions with stage 1 carbonate form under precipitation regimes of 1100––1300 mm/year (Shrivastava et al., 2002). Modern calcic soils on the Serengeti of Tanzania (~1–5°S) under monsoonal conditions show a similar relationship between carbonate buildup and precipitation. Carbonate nodules become rarer as precipitation approaches 1100 mm/year (Jager, 1982). Modern precipitation values suggest that during PFM deposition, therapsid inceptisols and calcic inceptisols formed under an annual precipitation of ~1100–1300 mm/year.

Precipitation played a large role in influencing *Camborygma Vertisol* ichnopedofacies development. In contemporary central India (~20–30°N), vertisols are found under precipitation regimes of 500–1300 mm/yr (Shrivastava *et al.*, 2002). These vertisols also display various levels of carbonate buildup, with heavy carbonate dissolution occurring in vertisols where annual precipitation is 1000–1300 mm (Shrivastava *et al.*, 2002). The lack of carbonate in the *Camborygma* Vertisol suggests (1) precipitation levels were >1300 mm/yr, precluding carbonate formation, and (2) a shift to more humid conditions across the PFM–ORM transition.

Differences in carbonate development between the two types of lower ORM calcic alfisol ichnopedofacies was not due to differences in duration of pedogenesis, but variations in precipitation levels. Modern soils with stage 2 carbonate under monsoonal conditions form on the Serengeti Plain (~1–5°S) under precipitation regimes from 700–1100 mm/yr (Jager, 1982). This suggests *Naktodemasis* calcic alfisols formed under an annual precipitation of ~700–1100 mm. Modern soils with stage 3 car-

bonate similar in size to those in the rhizolith calcic alfisols are found in southern India (~10–12°N) under precipitation regimes of 400–500 mm/yr (Shankar and Achyuthan, 2007). Carbonate nodules are also present throughout the whole profile of modern calcic soils forming under monsoonal conditions in central India (~20–30°N) under precipitation regimes of 500–700 mm/yr (Shrivastava *et al.*, 2002). This suggests the rhizolith calcic alfisols formed under an annual precipitation of ~400–700 mm. Thick Btk horizons in the lower ORM also suggest smaller scale cycles of decreasing precipitation, allowing the top of the calcic horizon to move upward over time (Birkeland, 1999). Higher precipitation allows water to flow deeper into the soil profile, washing out and dissolving the carbonate nodules (Gile *et al.*, 1966; Shrivastava *et al.*, 2002). Preservation of thick calcic horizons indicates precipitation decreased and rainfall reached shallower and shallower levels, recording small-scale drying cycles during monsoonal conditions. The change from *Camborygma* vertisols to *Naktodemasis* calcic alfisols to rhizolith calcic alfisols marks a clear shift to drier conditions during lower ORM deposition, from >1300 mm/yr to ~700–1100 mm/yr to finally ~400–700 mm/yr.

In the middle ORM, ichnopedofacies shift to *Camborygma* inceptisols and calcic inceptisols (Figs 4, 12). *Camborygma* likely formed during annual precipitation of ~1100 mm (Jager, 1982); stage 2 carbonate then formed and moved upward in the profile as precipitation dropped towards ~700 mm/yr. Despite a decrease in precipitation during formation of the *Camborygma* inceptisols and calcic inceptisols, precipitation levels were still higher than during formation of the rhizolith calcic alfisols lower in the section. The reappearance of *Camborygma* at the top of the middle ORM suggests a return to precipitation levels of ~1100 mm/yr heading into the middle ORM-upper ORM contact.

Ichnopedofacies shift to *Naktodemasis* alfisols and *Naktodemasis* inceptisols and calcic inceptisols in the upper ORM (Figs 4, 12). Precipitation levels were likely ~1100 mm/yr at the base of the upper ORM, then decreased to ~700 mm/yr up section. Increasing sediment deposition during drier climate, however, shortened the duration of pedogenesis and precluded formation of more numerous carbonates in these ichnopedofacies.

Ichnopedofacies shift from *Naktodemasis* inceptisols and calcic inceptisols to rhizolith inceptisols and shallowly burrowed entisols in the CRM, indicating a change from high, steady sedimentation to higher, nonsteady sedimentation rates and shorter duration of pedogenesis (Figs 4, 12; Kraus, 1999; Hasiotis and Platt, 2012). Sediment reworking by meandering and braided rivers, frequent overbank flooding, and proximity to the fluvial channel prevented the formation of better developed palaeosols and deeper penetrating organisms higher in the member. Shallowly burrowed entisols associated with playa lake deposits are similar to modern shallow playa lakes in Australia (~35°S) that form under a precipitation regime of 325 mm/yr (Teller and Last, 1990). This comparison suggests that shallowly burrowed entisols in playa lake deposits formed under an annual precipitation of ~325 mm. Rhizoliths in CRM ichnopedofacies give a lower limit for precipitation levels. In the modern Namib

desert of Namibia (~23–24°S), the precipitation limit of vegetated surfaces is ~25 mm/yr (Amit *et al.*, 2010). This suggests mean annual precipitation towards the end of CRM deposition was ~325–25 mm. The shift from *Naktodemasis* inceptisols and calcic inceptisols to shallowly burrowed entisols and rhizolith inceptisols suggests precipitation levels decreased from ~400 mm/yr to ~325–25 mm/yr, and that moisture still entered the environment until the very end of Chinle Fm deposition (Dubiel, 1987; Dubiel *et al.*, 1991; Dubiel and Hasiotis, 2011).

Hydrology: Groundwater and soil moisture conditions, influenced by climate and proximity to alluvial and lacustrine systems (Hasiotis, 2002, 2004, 2008; Hasiotis *et al.*, 2007a, 2012), varied during Chinle FM deposition, affecting stratigraphic distribution of ichnofossils and depths of burrowing (Figs 4, 12). The wettest intervals are the PFM, base of the lower ORM, base and top of the middle ORM, and base of the upper ORM. These units also have the greatest occurrences of *Camborygma*, which penetrate below the water table into the phreatic zone (Hasiotis and Mitchell, 1993; Hasiotis *et al.*, 1993; Hasiotis, 2002). Higher precipitation in the PFM, base of the lower ORM, base and top of the middle ORM, and base of the upper ORM resulted in a shallower water table, and more common burrowing by crayfish. Times of decreased precipitation outside of these intervals, however, resulted in deepened water tables, and less common burrowing by crayfish. No *Camborygma* is present in the CRM; precipitation was too low and the water table was too deep for *Camborygma* to form. An overall decrease in the water table during Chinle Fm deposition caused *Camborygma* to occur less often up section and have greater burrowing depths.

The only instances where hydrophilic and hygrophilic behaviour, including *Camborygma*, occurred during times of decreased precipitation are in levee deposits in the middle and upper ORM. Restriction of deep burrowing to proximal deposits and the predominance of hygrophilic behaviours indicate fluvial systems fed the groundwater in CRM time.

Ichnofossils displaying terraphilic behaviour become more dominant up section during Chinle Fm deposition (Figs 4, 12). In the PFM, lower ORM, and middle ORM, a variety of ichnofossils displaying all four burrowing behaviour categories are observed in floodplain and palustrine deposits. By upper ORM deposition, *Naktodemasis* and root ichnofossils dominate palaeosol profiles. Root ichnofossils become the only ichnofossils present in floodplain deposits in the CRM. Decreasing water tables through Chinle Fm deposition – due to decreasing precipitation levels – expanded the vadose zone and created conditions favourable to terraphilic burrowers. By CRM deposition, soil moisture conditions became too dry to support organisms other than occasional plants.

CLIMATIC VARIATION IN THE CHINLE BASIN

Numerous investigations support increasing aridity throughout Chinle Fm deposition, but there is disagreement concerning the details and cause of this climate shift

(Blakey and Gubitosa, 1983; Dubiel *et al.*, 1991; Prochnow *et al.*, 2006a; Cleveland *et al.*, 2008a, b; Dubiel and Hasiotis, 2011; Atchley *et al.*, 2013; Nordt *et al.*, 2015). Previous studies corroborate a transition from humid to subhumid and semiarid conditions during deposition of the PFM (Prochnow *et al.*, 2006a; Cleveland *et al.*, 2008a). Atchley *et al.* (2013) and Nordt *et al.* (2015) suggested this climate transition resulted in complete collapse of the Pangean megamonsoon due to uplift of the Cordilleran magmatic arc. Nordt *et al.* (2015) also cites magnetostratigraphic studies that suggest Pangea remained in the tropics throughout Chinle Fm deposition (Steiner and Lucas, 2000; Loope *et al.*, 2004; Rowe *et al.*, 2007; Zeigler and Geissman, 2011). This explanation is in contrast to Dubiel (1987, 1989) and Dubiel *et al.* (1991), who interpreted a monsoonal climate that persisted until the end of the Late Triassic with a decrease in precipitation caused by the northward movement of Pangea.

Monsoonal indicators in ichnopedofacies of the PFM and ORM in this study indicate that palaeomonsoon circulation did not collapse during deposition of either of these members. Playa lake, braided river, and meandering river deposits in the CRM further suggest strongly seasonal moisture until the end of Chinle Fm deposition, supporting the continuation of monsoonal conditions until the end of the Triassic. Gradual drying was likely due to the migration of Pangea into the midlatitudes (Dubiel *et al.*, 1991; Dubiel and Hasiotis, 2011).

Research in the Chinle Basin of alluvial and lacustrine deposits did not identify any Milankovitch cyclicity (e.g., Prochnow *et al.,* 2006a; Cleveland *et al.*, 2008a; Atchley *et al.*, 2013; Nordt *et al.*, 2015; this study). Olsen and Kent (1996, 1999), Olsen *et al.* (1996), and Olsen (1997) identified precession cycles nested within eccentricity cycles in Upper Triassic lacustrine deposits of the Newark Basin. The lack of well-preserved Milankovitch cyclicity in north-east Chinle Basin ichnopedofacies of the MM, PFM, ORM, and CRM can be attributed to: (1) autocyclic channel migration and overbank flooding episodes that produced variable duration of pedogenesis; and (2) the cut and fill nature of deposits obscured the preservation of cycles throughout the entire formation.

Climate indicators suggest wet-dry patterns in precipitation across the Chinle Basin. In eastern Utah, Prochnow *et al.* (2006a) suggested precipitation decreased from >1400 mm/yr to ~400 mm/yr during PFM deposition, and increased from ~400 mm/yr to ~600 mm/yr during deposition of the ORM and CRM. Atchley *et al.* (2013) and Nordt *et al.* (2015) interpreted highly fluctuating moisture conditions during deposition of the upper PFM and ORM at PFNP and the surrounding vicinity, with highs of ~1000 mm/yr during wet periods and lows of ~200 mm/yr during dry periods. Nordt *et al.* (2015) additionally identified a humid period with mean annual precipitation (MAP) of ~900 mm near the base of the ORM. In northern New Mexico, Cleveland *et al.* (2008a) determined MAP between ~200–450 mm for PFM to RPM deposition, and the RPM contained wet-dry fluctuations. This research, however, did not address the mechanism behind these wet-dry cycles, instead it focused on longer term climatic trends and controls

(Cleveland *et al.*, 2008a; Atchley *et al.*, 2013; Nordt *et al.*, 2015).

These low MAP values are at odds with the location of the Chinle Basin in sub-30° palaeolatitudes under a megamonsoonal regime in greenhouse conditions (Dickinson, 1981; Parrish and Peterson, 1988; Bazard and Butler, 1991; Dubiel *et al.*, 1991; Dubiel, 1994; Dubiel and Hasiotis, 2011). They are also lower than precipitation values for modern, near-equatorial environments affected by monsoons, such as the Serengeti plains of Tanzania (e.g., Oliver, 1973; Jager, 1982; Lydolph, 1985; Aber and Melillo, 1991; Sinclair *et al.*, 2007) and central India (e.g., Shrivastava *et al.*, 2002; Shankar and Achyuthan, 2007).

Estimated precipitation values determined in our study of the north-east Chinle Basin by utilizing ichnopedofacies and modern environmental and latitudinal analogues (Fig. 4) are, in general, higher than MAP values determined through geochemical methods alone in previous research elsewhere in the Chinle Basin. For the PFM, Prochnow *et al.* (2006a), Atchley *et al.* (2013), and Nordt *et al.* (2015) do have precipitation estimates of ~1000 mm/yr, and even up to ~1400 mm/yr in the case of Prochnow *et al.* (2006a). Their MAP estimates are similar to the ~1100–1300 mm/yr precipitation levels determined in our study. Cleveland et al. (2008a), however, only estimated ~200–450 mm MAP for PFM equivalent deposits, well below our estimates for the north-east Chinle Basin. For ORM deposits in eastern Utah, the estimated ~400–500 mm MAP by Prochnow *et al.* (2006a) is significantly lower than the ~400–1300 mm/yr range in precipitation levels suggested by ichnopedofacies. Atchley *et al.* (2013) and Nordt *et al.* (2015), however, estimate MAP up to ~1000 mm/yr during wet intervals in the ORM at PFNP, which is within our range of estimates for the north-east Chinle Basin. Their MAP estimates for dry intervals, however, are as low as ~200 mm/yr, which is half of the estimates based on ichnopedofacies. Cleveland *et al.* (2008a) has even lower precipitation estimates for the Chinle Fm in New Mexico. Palaeosols in the RPM at Ghost Ranch have estimated MAP of ~200–450 mm based on depth-to-carbonate functions. These palaeosols also exhibit gleyed soil matrix, wedge-shaped peds, abundant semiplasmic fabrics, and *Camborygma eumekenomos* 20–80 cm deep that are lined with carbonate nodules. These palaeosols have similar appearance to *Camborygma* calcic inceptisols in the north-east Chinle Basin, with an estimated MAP of ~700–1100 mm.

These variations in MAP interpretations highlight the importance to integrate ichnological and pedogenic features–to create ichnopedofacies–into palaeoprecipitation estimates that are correlated to modern environmental and latitudinal analogues in order to build more accurate climate models. The main reason for this variation is the use of different indicators to estimate annual precipitation. Some of these studies did attempt to assign modern soil classifications to palaeosols, but none combined both the ichnological and pedogenical features, nor compared palaeosols to modern environmental, behavioural, and latitudinal analogues. Prochnow *et al.* (2006a), Atchley *et al.* (2013), and Nordt *et al.* (2015) used geochemical weathering indices to calculate MAP, but did not incorporate ichnological evidence into

their estimates. Cleveland *et al.* (2008a), while incorporating some pedogenic and ichnological features, determined MAP using depth-to-carbonate functions (DTCF), and stated that, as a consequence, MAP values were likely minimum estimates. Prochnow *et al.* (2006a) also used DTCF for some MAP estimates.

Despite the use of different climate indices, overall trends of palaeoprecipitation variation across the Chinle Basin are recognized. Although MAP values from New Mexico palaeosols may be underestimates, the lack of *Camborygma* from PFM equivalent units does suggest lower water tables and decreased precipitation was present south of the north-east Chinle Basin during this time period. An east–west trend in precipitation values is also recognized. In the north-east Chinle Basin, a *Camborygma* Vertisol is observed within the lower ORM at south-west section(Figs 4, 12), and represents the highest precipitation levels in our study area at >1300 mm/yr. This ichnopedofacies appears to occur in the same stratigraphic interval as the 900 mm/yr humid pulse at PFNP, which falls well within the precipitation estimates from our study. Both the centre and north-east edge of the Chinle Basin contain evidence for a pulse of wetter conditions, but estimated precipitation was higher during the wetter interval in the north-east Chinle Basin. Precipitation levels in the north-east Chinle Basin varied from levels at the south-east edge and centre of the basin. Climatic conditions were, therefore, not consistent across the Chinle Basin during the Late Triassic.

CONCLUSIONS

Twelve ichnopedofacies, constructed from seventeen ichnofossil morphotypes and six palaeosol orders, were identified in the Chinle Fm of the north-east Chinle Basin: 1) Shallowly burrowed entisols; 2) rhizolith entisols; 3) *Camborygma* entisols; 4) *Naktodemasis-Camborygma* entisols; 5) rhizolith inceptisols; 6) *Naktodemasis* inceptisols and calcic inceptisols; 7) *Camborygma* inceptisols and calcic inceptisols; 8) Therapsid inceptisols and calcic inceptisols; 9) *Camborygma* vertisols; 10) *Naktodemasis* alfisols; 11) *Naktodemasis* calcic alfisols; and 12) rhizolith calcic alfisols.

Ichnopedofacies development and their lateral and vertical distribution reveal that the north-east Chinle Basin was influenced by a variety of physiochemical controls:

1. Higher frequency of channel migration and overbank flooding in the MM resulted in poorly developed and preserved ichnopedofacies. Reduced influence of autocyclic processes in the PFM and lower ORM resulted in more developed, calcic ichnopedofacies. Increasing frequency of autocyclic events during middle ORM deposition resulted in a transition from composite, calcic ichnopedofacies at the base of the unit to less developed, compound, non-calcic alfisols and inceptisols between channel migration and overbank flooding deposits. Frequency of autocyclic events decreased during the upper ORM, resulting in the formation of more developed cumulative and composite, calcic ichnopedofacies. Increasing frequency of channel migration and overbank flooding in the CRM resulted in a shift from more developed, calcic

ichnopedofacies to poorly developed, compound inceptisols and entisols.

2. Basin subsidence controlled the development of fluvial systems. Sand sheets of braided river deposits suggest decreased subsidence, decreased accommodation, frequent fluvial reworking, and reduced duration of pedogenesis in the MM. A shift to ribbon sand bodies in the PFM and ORM suggest meandering rivers with increased subsidence, increased accommodation, less fluvial reworking and greater duration of pedogenesis. Sheet and ribbon sand deposits in the CRM suggest a decrease in basin subsidence, leading to decreased accommodation, more fluvial reworking, and shorter duration of pedogenesis. Ribbon sand deposits in the CRM, however, indicate accommodation was still greater than in the MM, allowing for the preservation of playa lake deposits.

3. Changes in base level cut and filled palaeovalleys, preserving the palaeotopography present during Chinle Fm deposition. Topographic position and changes in rate of valley fill influenced ichnopedological development. High, nonsteady sedimentation and decreased accommodation in the MM resulted in compound entisols. Low, nonsteady sedimentation during PFM and lower ORM deposition resulted in more developed, compound and composite ichnopedofacies. An increase in nonsteady sedimentation led to more frequent autocyclic deposits in the middle ORM and a transition from composite, calcic ichnopedofacies to compound and composite, non-calcic ichnopedofacies. Sedimentation rate slightly decreased and shifted to steady state sedimentation in the upper ORM, resulting in cumulative and composite ichnopedofacies. A shift back to nonsteady sediment deposition in the CRM and increasing sedimentation rates resulted in a transition from composite, calcic ichnopedofacies to compound entisols and inceptisols. Overall, a south to north trend of decreasing rates of valley fill is observed in the PFM, lower ORM, and upper ORM.

4. Salt tectonism led to the uplift and cannibalization of lacustrine deposits. Increased accommodation in the lower ORM enabled the formation of lakes with oncoids. Following halokinetic uplift and erosion, oncoids were redeposited in laterally accreted conglomerate beds, remaining the only indicator of previous lacustrine systems in the study area.

5. Climate overall became drier during Chinle Fm deposition with multiple smaller wet-dry cycles. This pattern is reflected in the alternations between calcic and non-calcic ichnopedofacies, and polygenetic palaeosol formation with calcium carbonate nodules overprinting gleyed horizons and ichnofossils.

6. Groundwater and soil moisture conditions largely mirror changes in climate. The water table, influenced by precipitation, decreased up section during Chinle Fm deposition, and ichnofossils reflecting hydrophilic and hygrophilic behaviours also decreased up section. Ichnofossils displaying hydrophilic and hygrophilic behaviours during periods of decreased precipitation indicate a shallower water table fed by nearby rivers. No ichnofossils displaying hydrophilic behaviour are present in the CRM; instead hygrophilic behaviour is observed in

levee deposits where local water tables were higher. Ichnofossils displaying terraphilic behaviour become more dominant up section, and root ichnofossils become the only ichnofossils observed in CRM deposits. *Naktodemasis* overprinting the burrow fill of *Camborygma* in ORM and CRM fluvial deposits reflect drops in the water table following flooding events or small-scale drying cycles.

Signatures of seasonality and decreasing precipitation are seen throughout Chinle Fm deposition in the north-east Chinle Basin.

1. Therapsid inceptisols and calcic inceptisols in the PFM suggest an annual precipitation of ~1100–1300 mm with carbonate buildup during drier periods.

2. *Camborygma* vertisols in the lower ORM indicate highly seasonal precipitation >1300 mm/yr with fluctuating water tables. Thick Btk horizons with stage 2–3 carbonate in overlying *Naktodemasis* calcic alfisols and rhizolith calcic alfisols indicate a decrease in precipitation from ~700–1100 mm/yr to ~400–700 mm/yr and short-term drying cycles.

3. *Camborygma* inceptisols and calcic inceptisols in the middle ORM suggest highly fluctuating water tables and a decrease in annual precipitation from ~1100 mm to ~700 mm. Reappearance of *Camborygma* at the top of the middle ORM indicates precipitation increased to ~1100 mm/yr heading into the upper ORM.

4. Transition to *Naktodemasis* alfisols and *Naktodemasis* inceptisols and calcic inceptisols in the upper ORM suggests another drying cycle from ~1100 mm/yr to ~700 mm/yr.

5. *Naktodemasis* inceptisols and calcic inceptisols near the base of the CRM suggest precipitation levels of ~400 mm/yr. Rhizolith inceptisols and playa lake deposits with shallowly burrowed entisols suggest a precipitation decrease to ~325–25 mm/yr near the end of Chinle Fm deposition. Despite extended dry periods, the presence of braided river, meandering river, and playa lake deposits indicate that moisture was still present until the end of the Triassic.

Ichnopedofacies suggest monsoonal circulation continued throughout Chinle Fm deposition and did not fully collapse until the end of the Triassic Period and the migration of Wingate Sandstone eolian dunes into the area of the Colorado Plateau.

The Late Triassic in the Chinle Basin was characterized by complex climatic patterns which greatly influenced local depositional environments, palaeotopography, hydrology, pedogenic development, and ichnofossil distribution. Most variation in estimates of precipitation levels across the Chinle Basin can be attributed to the use of different climate indices between studies. The use of ichnopedofacies and modern soil, environmental, behavioural, and latitudinal analogues in our study resulted in higher MAP values in general than previous studies of the Chinle Basin, which utilized geochemical weathering indices and depth-to-carbonate functions. Variations between MAP values highlights the need to incorporate ichnopedological features and modern environmental, behavioural, and latitudinal analogues into precipitation estimates to develop more accurate climate models. MAP estimates from previous studies are too low

for the interpretation of the Chinle Basin being deposited in sub-30° palaeolatitudes under a megamonsoonal regime in greenhouse conditions.

This is the first study to establish ichnopedofacies in the Chinle Fm. Ichnopedofacies have proved to be useful tools for interpreting fine-scale sedimentological, hydrological, and climatic conditions of Chinle Fm deposits. Future use in other Chinle Fm localities will aid in working out detailed interpretations of the timing of climatic changes and cyclicity in precipitation and will further the understanding of the spatial and temporal variations in climatic conditions in the south-west United States during the Late Triassic. Ichnopedofacies, however, are not confined for use only in the Chinle Fm. There is great potential in expanding ichnopedofacies to other continental strata.

REFERENCES

Abell, P. I., Awramik, S. M., Osborne, R. H. & Tomellini, S., 1982. Plio-Pleistocene lacustrine Stromatolites from Lake Turkana, Kenya: Morphology, stratigraphy, and stable isotopes. *Sedimentary Geology*, 32: 1–26.

Aber, J. D. & Melillo, J.M., 1991. *Terrestrial Ecosystems*. Saunders, Philadelphia, PA, 429 pp.

Alexander, J. & Leeder, M. R., 1987. Active tectonic controls in alluvial architecture. In: Ethridge, F. G., Flores, R. M. & Harvey, M. D. (eds), *Recent Developments in Fluvial Sedimentology*. SEPM Special Publication, 39: 243–252.

Allen, J. R. L., 1970. Studies in fluviatile sedimentation: A comparison of fining-upwards cyclothems, with special references to coarse-member composition and interpretation. *Journal of Sedimentary Petrology*, 40: 298–323.

Alonso-Zara, A. M., Genise, J. F. & Verde, M., 2014. Palaeoenvironments and ichnotaxonomy of insect trace fossils in continental mudflat deposits of the Miocene Calatayud-Daroca Basin, Zaragoza, Spain. *Palaeogeography, Palaeoclimatology, Palaeoecology*, 414: 342–351.

Amit, R., Enzel, Y., Grodek, T., Crouvi, O., Porat, N. & Ayalon, A., 2010. The role of rare rainstorms in the formation of calcic soil horizons on alluvial surfaces in extreme deserts. *Quaternary Research*, 74: 177–187.

Arenas, C., Cabrera, L. & Ramos, E., 2007. Sedimentology of tufa facies and continental microbialites from the Palaeogene of Mallorca Island (Spain). *Sedimentary Geology*, 197: 1–27.

Ash, S. R. & Hasiotis, S. T., 2013. New occurrences of the controversial Late Triassic plant fossil *Sanmiguelia* Brown and associated ichnofossils in the Chile Formation of Arizona and Utah, USA. *Neues Jahrbuch für Geologie und Paläontologie, Abhandlungen,* 268: 65–82.

Atchley, S. C., Nordt, L. C., Dworkin, S. I., Ramezani, J., Parker, W. G., Ash, S. R. & Bowring, S. A., 2013. A linkage among Pangean tectonism, cyclic alluviation, climate change, and biologic turnover in the Late Triassic: The record from the Chinle Formation, southwestern United States. *Journal of Sedimentary Research*, 83: 1147–1161.

Bazard, D. R. & Butler, R. F., 1991. Paleomagnetism of the Chinle and Kayenta Formations, New Mexico and Arizona. *Journal of Geophysical Research*, 96: 9847–9871.

Beerbower, J. R., 1964. Cyclothems and cyclic depositional mechanisms in alluvial plain sedimentation. In: Merriam, D. F. (ed.), *Symposium on Cyclic Sedimentation: State Geological Survey of Kansas Bulletin*, 2: 31–42.

Birkeland, P. W., 1999. *Soils and Geomorphology, Third Edition*. Oxford University Press, New York, 430 pp.

Blakey, R. C., 1989. Triassic and Jurassic geology of the southern Colorado Plateau. In: Jenny, J. P. & Reynolds, S. J. (eds), *Geologic Evolution of Arizona. Geological Society Digest*, 17: 369–396, Tucson, Arizona.

Blakey, R. C. & Gubitosa, R., 1983. Late Triassic palaeogeography and depositional history of the Chinle Fm, southern Utah and northern Arizona. In: Reynolds, M. W. & Dolly, E. D. (eds), *Mesozoic palaeogeography of the west-central United States, Rocky Mountain Paleogeography Symposium 2*. The Rocky Mountain Section, SEPM, Denver, pp. 57–76.

Blakey, R. C. & Gubitosa, R., 1984. Controls of sandstone body geometry and architecture in the Chinle Formation (Upper Triassic), Colorado Plateau. *Sedimentary Geology*, 38: 51–86.

Bohacs, K., Hasiotis, S. T., & Demko, T. M., 2007. Continental ichnofossils of the Green River and Wasatch Formations, Eocene, Wyoming: a preliminary survey, proposed relation to lake-basin types, and application to integrated paleoenvironmental interpretation. *The Mountain Geologist*, 44(2): 79-108.

Bown, T. M. & Kraus, M. J., 1987. Integration of channel and floodplain suites, I. Developmental sequence and lateral relations of alluvial palaeosols. *Journal of Sedimentary Petrology*, 57: 587–601.

Bown, T. M. & Kraus, M. J., 1993a. Time-stratigraphic reconstruction and integration of palaeopedologic, sedimentologic, and biotic events (Willwood Formation, Lower Eocene, northwest Wyoming, U.S.A.). *Palaios*, 8: 66–80.

Bown, T. M. & Kraus, M. J., 1993b. Soils, time, and primate palaeoenvironments. *Evolutionary Anthropology*, 2: 11–21.

Brewer, R., 1976. *Fabric and Mineral Analysis of Soils, 3rd Edition*. Kreiger, New York, 470 pp.

Bridge, J. S., 1984. Large-scale facies sequences in alluvial overbank environments. *Journal of Sedimentary Petrology*, 54: 583–588.

Bridge, J. S. & Leeder, M. R., 1979. A simulation model of alluvial stratigraphy. *Sedimentology*, 26: 617–644.

Bromley, R. G., 1996. *Trace Fossils: Biology, Taphonomy, and Applications, 2nd Edition*. Chapman and Hall, London, 361 pp.

Bromley, R. G. & Asgaard, U., 1979. Triassic freshwater ichnocoenoses from Carlsberg Fjord, east Greenland. *Palaeogeography, Palaeoclimatology, Palaeoecology*, 28: 39–80.

Cater, F. W., 1970. Geology of the Salt Anticline Region in southwestern Colorado. *Geological Survey Professional Paper*, 637: 1–80.

Cecil, C. B., 2003. The concept of autocyclic and allocyclic controls on sedimentation and stratigraphy, emphasizing the climatic variable. In: Cecil, C. B. & Edgar, T. N. (eds), *Climate Controls on Stratigraphy*. SEPM Special Publication, 77: 13–20.

Cleveland, D. M., Atchley, S. C. & Nordt, L. C., 2007. Continental sequence stratigraphy of the Upper Triassic (Norian-Rhatian) Chinle strata, northern New Mexico, USA: Allocyclic and autocyclic origins of palaeosols-bearing alluvial successions. *Journal of Sedimentary Research*, 77: 909–924.

Cleveland, D.M., Nordt, L.C. & Atchley, S.C., 2008a. Paleosols, trace fossils, and precipitation estimates of the uppermost Triassic strata in northern New Mexico. *Palaeogeography, Palaeoclimatology, Palaeoecology*, 257: 421–444.

Cleveland, D. M., Nordt, L. C., Atchley, S. C. & Dworkin, S., 2008b. Pedogenic carbonate isotopes as evidence for extreme climate events preceding the Triassic-Jurassic boundary: Implications for the biotic crisis? *Geological Society of America Bulletin*, 120: 1408–1415.

Collinson, J. D., 1986. Alluvial sediments. In: Reading, H. G. (ed.), *Sedimentary Environments and Facies, 2nd Edition*. Blackwell Scientific Publication, Oxford, pp. 20–62.

Compton, R. R., 1985. *Geology in the Field*. John Wiley & Sons, Inc., New York, 398 pp.

Counts, J. W. & Hasiotis, S. T., 2009. Neoichnological experiments with masked chafer beetles (Coleoptera: Scarabaeidae): Implications for backfilled continental trace fossils. *Palaios*, 24: 74–91.

Counts, J. W. & Hasiotis, S. T., 2014. Distribution, palaeoenvironmental implications, and stratigraphic architecture of palaeosols in Lower Permian continental deposits of western Kansas, U.S.A. *Journal of Sedimentary Research*, 84: 144–167.

Dickinson, W. R., 1981. Plate Tectonic evolution of the southern Cordillera. In: Dickinson, W. R. & Payne, W. D. (eds), *Relations of Tectonics to Ore Deposits in the Southern Cordillera. Arizona Geological Society Digest*, 14: 113–135.

Dickinson, W. R. & Gehrels, G. E., 2008. U-Pb ages of detrital zircons in relation to palaeogeography: Triassic palaeodrainage networks and sediment dispersal across southwest Laurentia. *Journal of Sedimentary Research*, 78: 745–764.

Driese, S. G. & Foreman J. L., 1992. Paleopedology and palaeoclimatic implications of Late Ordovician vertic palaeosols, Juniata Formation, southern Appalachians. *Journal of Sedimentary Petrology*, 62: 71–83.

Driese, S. G. & Mora, C. I., 1993. Physico-chemical environment of pedogenic carbonate formation in Devonian vertic palaeosols, central Appalachians, USA. *Sedimentology*, 40: 199–216.

Driese, S. G. & Mora, C. I., 2002. Paleopedology and stable isotope geochemistry of Late Triassic (Carnian–Norian) palaeosols, Durham Sub-basin, North Carolina, U.S.A. Implications for palaeoclimate and palaeoatmospheric PCO_2. In: Renaut, R. W. & Ashley, G. M. (eds), *Sedimentation in Continental Rifts. SEPM Special Publication*, 73: 207–218.

Driese, S. G., Simpson E. L. & Eriksson, K. A., 1995. Redoximorphic palaeosols in alluvial and lacustrine deposits, 1.8 GA Lochness Formation, Mount Isa, Australia: Pedogenic processes and implications for palaeoclimate. *Journal of Sedimentary Research*, A65: 675–689.

Dubiel, R. F., 1987. Sedimentology of the Upper Triassic Chinle Fm, southeastern Utah – Paleoclimatic implications. In: Morales, M. & Elliott, D. K. (eds), *Triassic Continental Deposits of the American Southwest. Journal of the Arizona-Nevada Academy of Science*, 22: 35–45.

Dubiel, R. F., 1989. Depositional and climatic setting of the Upper Triassic Chinle Fm, Colorado Plateau. In: Lucas, S. G. & Hunt, A. P. (eds), *Dawn of the Age of Dinosaurs in the American Southwest*. New Mexico Museum of Natural History, Albuquerque, pp. 171–187.

Dubiel, R. F., 1994. Triassic deposystems, palaeogeography, and palaeoclimate of the Western Interior. In: Caputo, M. V., Peterson, J. A. & Franczyk, K. J. (eds), *Mesozoic Systems of the Rocky Mountain Region, USA*. SEPM (Society for Sedimentary Geology), Rocky Mountain Section, Denver, pp. 133–168.

Dubiel, R. F. & Hasiotis, S. T., 2011. Deposystems, palaeosols, and climatic variability in a continental system: The Upper Triassic Chinle Fm, Colorado Plateau, USA. In: Davidson, S. K., Leleu, S. & North, C. P. (eds), *From River to Rock Record: The Preservation of Fluvial Sediments and their Subsequent Interpretation. SEPM Special Publication,* 97: 393–421.

Dubiel, R. F., Good, S. C. & Parrish, J. M., 1989. Sedimentology and Paleontology of the Upper Triassic Chinle Formation, Bedrock, Colorado. *The Mountain Geologist*, 26: 112–125.

Dubiel, R. F., Parrish, J. T., Parrish, J. M. & Good, S. C., 1991. The Pangaean megamonsoon– Evidence from the Upper Triassic Chinle Fm, Colorado Plateau. *Palaios*, 6: 347–370.

Dubiel, R. F., Skipp, G. & Hasiotis, S. T., 1992. Continental depositional environments and tropical palaeosols in the Upper Triassic Chinle Fm, Eagle Basin, western Colorado. In: Flores, R. M. (ed.), *SEPM Mid-Year Meeting on the Mesozoic of the Western Interior, Fieldtrip Guidebook*. SEPM, Fort Collins, Colorado, pp. 21–37.

Frey, R. W., Pemberton, S. G. & Fagerstrom, J. A., 1984. Morphological, ethological, and environmental significance of the ichnogenera *Scoyenia* and *Ancorichnus*. *Journal of Paleontology*, 58: 511–528.

Gaston, R., Lockley, M. G., Lucas, S. G. & Hunt, A. P., 2003. *Grallator*–dominated fossil footprint assemblages and associated enigmatic footprints from the Chinle Group (Upper Triassic), Gateway area, Colorado. *Ichnos*, 10: 153–163.

Getty, P. R., McCarthy, T. D., Hsieh, S. & Bush, A. M., 2016. A new reconstruction of continental *Treptichnus* based on exceptionally preserved material from the Jurassic of Massachusetts. *Journal of Paleontology*, 90: 269–278.

Gile, L. H., Peterson, F. F. & Grossman, R. B., 1966. Morphological and genetic sequences of carbonate accumulation in desert soils. *Soil Science*, 101: 347–360.

Gillette, L., Pemberton, S. G. & Sarjeant, W., 2003. A Late Triassic invertebrate ichnofauna from Ghost Ranch, New Mexico. *Ichnos*, 10: 141–151.

Hammersburg, S., Hasiotis, S. T. & Robison, R. A., 2018. Ichnotaxonomic assessment of the middle Cambrian Spence Shale Member of the Langston Formation, Utah. *The University of Kansas Paleontological Contributions*, 20: 1–66.

Hasiotis, S. T., 1995. Crayfish fossils and burrows from the Upper Triassic Chinle Formation, Canyonlands National Park, Utah. In: Santucci, V. L. & McClelland, L. (eds), *National Park Service Paleontological Research, Technical Report NPS/NRPO/*

NRTR-95/16. National Park Service/Natural Resources Publication Office, Lakewood, Colorado, pp. 49–53.

Hasiotis, S. T., 2000. The invertebrate invasion and evolution of Mesozoic soil ecosystems: the ichnofossil record of ecological innovations. In: Gastaldo, R.A. & Dimichele, W.A. (eds), *Phanerozoic Terrestrial Ecosystems. Paleontological Society Short Course*, 6: 141–169.

Hasiotis, S. T., 2002. *Continental Trace Fossils*. SEPM. Short Course Notes Number 51. SEPM , Tulsa, Oklahoma, 132 pp.

Hasiotis, S. T., 2003. Complex ichnofossils of solitary and social soil organisms: understanding their evolution and roles in terrestrial palaeoecosystems. *Palaeogeography, Palaeoclimatology, Palaeoecology*, 192: 259–320.

Hasiotis, S. T., 2004. Reconnaissance of Upper Jurassic Morrison Formation ichnofossils, Rocky Mountain Region, USA: palaeoenvironmental, stratigraphic, and palaeoclimatic significance of terrestrial and freshwater ichnocoenoses. *Sedimentary Geology*, 167: 177–268.

Hasiotis, S. T., 2007. Continental ichnology: Fundamental processes and controls on trace fossil distribution. In: Miller, W. III. (ed.), *Trace Fossils — Concepts, Problems, Prospects*. Elsevier, Amsterdam, pp. 268–284.

Hasiotis, S. T., 2008. Reply to the comments by Bromley et al. of the paper "Reconnaissance of the Upper Jurassic Morrison Formation ichnofossils, Rocky Mountain Region, USA: Paleoenvironmental, stratigraphic, and palaeoclimatic significance of terrestrial and freshwater ichnocoenoses" by Stephen T. Hasiotis. *Sedimentary Geology*, 208: 61–68.

Hasiotis, S. T. & Bown, T. M., 1992. Invertebrate trace fossils: The backbone of continental ichnology. In: Maples, C. G. & West, R. R. (eds), *Trace Fossils*. Short Courses in Paleontology, Number 55. The Paleontological Society, Knoxville, pp. 64–101.

Hasiotis, S. T. & Demko T. M., 1996. Terrestrial and freshwater trace fossils, Upper Jurassic Morrison Formation, Colorado Plateau. In: Morales, M. (ed.), *The Continental Jurassic. Museum of Northern Arizona Bulletin*, 60: 355–370.

Hasiotis, S. T. & Dubiel, R. F., 1993a. Continental trace fossils of the Upper Triassic Chinle Formation, Petrified Forest National Park, Arizona. In: Lucas, S. G. & Morales, M. (eds), *The Nonmarine Triassic. The New Mexico Museum of Natural History and Science Bulletin*, 3: 175–178.

Hasiotis, S. T. & Dubiel, R. F., 1993b. Trace fossil assemblages in Chinle Formation alluvial deposits at the Tepees, Petrified Forest National Park, Arizona. In: Lucas, S. G. & Morales, M. (eds), *The Nonmarine Triassic. The New Mexico Museum of Natural History and Science Bulletin*, 3: G42–43.

Hasiotis, S. T. & Dubiel, R. F., 1994. Ichnofossil tiering in Triassic alluvial palaeosols: Implications for Pangean continental rocks and palaeoclimate. In: Embry, A. F., Beauchamp, B. & Glass, D. (eds), *Carboniferous to Jurassic Pangea: Global Environments and Resources. Canadian Society of Petroleum Geologists, Memoir,* 17: 311–317.

Hasiotis, S. T. & Dubiel, R. F., 1995a. Continental trace fossils, Petrified Forest National Park, Arizona: Tools for palaeohydrologic and palaeoecosystem reconstructions. In: Santucci, V. L. & McClelland, L. (eds), *National Park Service Paleontological Research, Technical Report NPS/NRPO/NRTR-95/16*. National Park Service/Natural Resources Publication Office, Lakewood, Colorado, pp. 82–88.

Hasiotis, S. T. & Dubiel, R. F., 1995b. Termite (Insecta: Isoptera) nest ichnofossils from the Triassic Chinle Formation, Petrified Forest National Park, Arizona. *Ichnos*, 4: 119–130.

Hasiotis, S. T. & Honey, J. G., 2000. Paleohydrologic and stratigraphic significance of crayfish burrows in continental deposits: Examples from several Paleocene Laramide basins in the Rocky Mountains. *Journal of Sedimentary Research*, 70: 127–139.

Hasiotis, S. T., Kraus, M. J. & Demko, T. M., 2007a. Climatic controls on continental trace fossils. In: Miller, W., III. (ed.), *Trace Fossils — Concepts, Problems, Prospects* Elsevier, Amsterdam, pp. 172–195.

Hasiotis, S. T. & Martin, A. J., 1999. Probable reptile nests from the Upper Triassic Chinle Formation, Petrified Forest National Park, Arizona. In: Santucci, V. L. & McClelland, L. (eds), *National Park Service Paleontological Research, Technical Report, NPS/NRGRD/GRDTR-99/03*. National Park Service/ Natural Resources Publication Office, Lakewood, Colorado, pp. 85–90.

Hasiotis, S. T. & Mitchell, C. E., 1993. A comparison of crayfish burrow morphologies: Triassic and Holocene fossil, palaeo- and neo-ichnological evidence, and the identification of their burrowing signatures. *Ichnos*, 2: 291–314.

Hasiotis, S. T., Mitchell, C. E. & Dubiel, R. F., 1993. Application of morphologic burrow interpretations to discern continental burrow architects: Lungfish or crayfish. *Ichnos*, 2: 315–333.

Hasiotis, S. T. & Platt, B. F., 2012. Exploring the sedimentary, pedogenic, and hydrologic factors that control the occurrence and role of bioturbation in soil formation and horizonation in continental deposits: an integrative approach. *The Sedimentary Record*, 10: 4–9.

Hasiotis, S. T., Platt, B. F., Hembree, D. I. & Everhart, M., 2007b. The trace-fossil record of vertebrates. In: Miller, W., III (ed.), *Trace Fossils — Concepts, Problems, Prospects*, Elsevier, Amsterdam, pp. 196–218.

Hasiotis, S. T., Platt, B. F., Reilly, M., Amos, K., Lang, S., Kennedy, D., Todd, D. A. & Michel, E., 2012. Actualistic studies of the spatial and temporal distribution of terrestrial and aquatic organism traces in continental environments to differentiate lacustrine from fluvial, eolian, and marine deposits in the geologic record. In: Baganz, O. W., Bartov, Y., Bohacs, K. & Nummedal, D. (eds), *Lacustrine sandstone reservoirs and hydrocarbon systems. AAPG Memoir,* 95: 433–489.

Hasiotis, S. T., Wellner, R. W., Martin, A. J. & Demko, T. M., 2004. Vertebrate burrows from Triassic and Jurassic continental deposits in North America and Antarctica: Their palaeoenvironmental and palaeoecological significance. *Ichnos*, 11: 103–124.

Hazel, J. E., Jr., 1994. Sedimentary response to intrabasinal salt tectonism in the Upper Triassic Chinle Fm, Paradox Basin, Utah. *U. S. Geological Survey Bulletin,* 2000-F: 1–34.

Hembree, D. I. & Hasiotis, S. T., 2008. Miocene vertebrate and invertebrate burrows defining compound palaeosols in the Pawnee Creek Formation, Colorado, U.S.A. *Palaeogeography, Palaeoclimatology, Palaeoecology*, 270: 349–365.

Hobbs, H. H. Jr., 1981. The crayfishes of Georgia. *Smithsonian Contributions to Zoology*, 318: 1–549.

Jager, T. J., 1982. *Soils of the Serengeti Woodlands, Tanzania*. Centre for Agricultural Publishing and Documentation, Wageningen, 239 pp.

Jenny, H., 1941. *Factors of Soil Formation: A System of Quantitative Pedology*. McGraw-Hill, New York, 281 pp.

Johnston, P. A., Eberth, D. A. & Anderson, P. K., 1996. Alleged vertebrate eggs from Upper Cretaceous redbeds, Gobi Desert, are fossil insect (Coleoptera) pupal chambers: *Fictovichnus* new ichnogenus. *Canadian Journal of Earth Sciences*, 33: 511–525.

Klappa, C. F., 1980. rhizoliths in terrestrial carbonates: classification, recognition, genesis and significance. *Sedimentology*, 27: 613–629.

Kraus, M. J., 1987. Integration of channel and floodplain suites II. Vertical relations of alluvial palaeosols. *Journal of Sedimentary Petrology*, 57: 602–612.

Kraus, M. J., 1999. Paleosols in clastic sedimentary rocks: Their geologic applications. *Earth Science Reviews*, 47: 41–70.

Kraus, M. J., 2002. Basin scale changes in floodplain palaeosols: Implications for interpreting fluvial architecture. *Journal of Sedimentary Research*, 72: 500–509.

Kraus, M. J. & Aslan, A., 1993. Eocene hydromorphic palaeosols: Significance for interpreting ancient floodplain processes. *Journal of Sedimentary Petrology*, 63: 453–463.

Kraus, M. J. & Hasiotis, S. T., 2006. Significance of different modes of rhizolith preservation to interpreting palaeoenvironmental and palaeohydrologic settings: Examples from Paleogene palaeosols, Bighorn Basin, Wyoming, U.S.A. *Journal of Sedimentary Research*, 76: 633–646.

Kraus, M. J. & Middleton, L. T., 1987a. Dissected palaeotopography and base-level changes in a Triassic fluvial system. *Geology*, 15: 18–21.

Kraus, M. J. & Middleton, L. T., 1987b. Contrasting architecture of two alluvial suites in different structural settings. In: Ethridge, F. G., Flores, R. M. & Harvey, M. D. (eds.), *Recent Developments in Fluvial Sedimentology. SEPM Special Publication*, 39: 253–262.

Kureck, A., 1996. Eintagsfliegen am Rhein: Zur Biologie von Ephoron virgo (Oliver, 1791). *Decheniana*, 35: 17–24.

Loope, D. B., Steiner, M. B., Rowe, C. M. & Lancaster, N., 2004. Tropical westerlies over Pangaean sand seas. *Sedimentology*, 51: 315–322.

Lydolph, P.E., 1985. *The Climate of Earth*. Rowman & Allanheld Publishers, Totowa, NJ, 386 pp.

Machette, M. N., 1985. Calcic soils of the southwestern United States. *Geological Society of America Special Paper*, 203: 1–21.

Mack, G. H., James, W. C. & Monger, H. C., 1993. Classification of palaeosols. *Geological Society of America Bulletin*, 105: 129–136.

Martin, A. J. & Hasiotis, S. T., 1998. Vertebrate tracks and their significance in the Chinle Formation (Late Triassic) Petrified Forest National Park, Arizona. In: Santucci, V. L. & McClelland, L. (eds), *National Park Service Paleontological Research, Technical Report NPS/NRGRD/GRDTR-98/01*. National Park Service/Natural Resources Publication Office, Lakewood, Colorado, p. 138–143.

Melchor, R. N., Bromley, R. G., & Bedatou, E., 2009. *Spongeliomorpha* in nonmarine settings: an ichnotaxonomic approach. *Earth and Environmental Science Transactions of the Royal Society of Edinburgh*, 100: 429–436. doi:10.1017/ S1755691009008056

Miall, A. D., 1996. *The Geology of Fluvial Deposits: Sedimentary Facies, Basin Analysis, and Petroleum Geology*. Springer-Verlag, Berlin, 582 pp.

Moore, D. M. & Reynolds, R. C., 1997. *X-Ray Diffraction and the Identification and Analysis of Clay Minerals, Second Edition*. Oxford University Press, New York, 378 pp.

Munsell®, 2009. *Soil Colour Book, Revised Edition*. [Unpaginated.]

Nordt, L., Atchley, S. & Dworkin, S., 2015. Collapse of the Late Triassic megamonsoon in western equatorial Pangea, present-day American southwest. *Geological Society of America Bulletin*, B31186–1.

Oliver, J. E., 1973. *Climate and Man's Environment: An Introduction to Applied Climatology*. Wiley, New York, 517 pp.

Olsen, P. E., 1997. Stratigraphic record of the Early Mesozoic breakup of Pangea in the Laurasia-Gondwana rift system. *Annual Review of Earth and Planetary Sciences*, 25: 337–401.

Olsen, P. E. & Kent, D. V., 1996. Milankovitch climate forcing in the tropics of Pangea during the Late Triassic. *Palaeogeography, Palaeoclimatology, Palaeoecology*, 122: 1–26.

Olsen, P. E. & Kent, D. V., 1999. Long-period Milankovitch cycles from the Late Triassic and Early Jurassic of eastern North America and their implications for the calibration of the Early Mesozoic time-scale and the long-term behaviour of the plants. *Philosophical Transactions of the Royal Society*, 357: 1761–1786.

Olsen, P. E., Kent, D. V., Cornet, B., Witte, W. K. & Schlische, R. W., 1996. High-resolution stratigraphy of the Newark rift basin (early Mesozoic, eastern North America). *Geological Society of America Bulletin*, 108: 40–77.

Parcerisa, D., Gomez-Gras, D. & Martin-Martin, J. D., 2006. Calcretes, oncolites, and lacustrine limestones in Upper Oligocene alluvial fans of the Montgat area (Catalan Coastal Ranges, Spain). In: Alonso-Zarza, A. M. & Tanner, L. H. (eds), *Paleoenvironmental Record and Applications of Calcretes and Palustrine Carbonates. Geological Society of America Special Paper,* 416: 105–118.

Parrish, J. T. & Peterson, F., 1988. Wind directions predicted from global circulation models and wind directions determined from eolian sandstones of the western United States – A comparison. *Sedimentary Geology*, 56: 261–282.

Pemberton, S. G. & Frey, R. W., 1982. Trace fossil nomenclature and the *Planolites-Palaeophycus* dilemma. *Journal of Paleontology*, 56: 843–881.

Pipiringos, G. N. & O'Sullivan, R. B., 1978. Principle unconformities in Triassic and Jurassic rocks, Western Interior United States – A preliminary study. *Geological Survey Professional Paper*, 1035-A: 1–29.

Prochnow, S. J., Nordt, L. C., Atchley, S. C. & Hudec, M. R., 2006a. Multi-proxy palaeosol evidence for Middle and Late Triassic climate trends in eastern Utah. *Palaeogeography, Palaeoclimatology, Palaeoecology*, 232: 53–72.

Prochnow, S. J., Nordt, L. C., Atchley, S. C., Hudec, M. & Boucher, T. E., 2005. Triassic palaeosol catenas associated with a salt-withdrawal minibasin in southeastern Utah, U.S.A. *Rocky Mountain Geology*, 40: 25–49.

Prochnow, S. J., Atchley, S. C., Boucher, T. E., Nordt, L. C. & Hudecs, M. R., 2006b. The influence of salt withdrawal subsidence on palaeosol maturity and cyclic fluvial deposition

in the Upper Triassic Chinle Formation, Castle Valley, Utah. *Sedimentology*, 53: 1319–1345.

Ratcliffe, B. C. & Fagerstrom, J. A., 1980. Invertebrate lebensspuren of Holocene floodplains: their morphology, origin and palaeoecological significance. *Journal of Paleontology*, 54): 614–630.

Retallack, G. J., 2001. *Soils of the Past: An Introduction to Paleopedology, 2nd Edition*. Blackwell Science, Oxford, 404 pp.

Riggs, N. R., Lehman, T. M., Gehrels, G. E. & Dickinson, W. R., 1996. Detrital zircon link between headwaters and terminus of the Upper Triassic Chinle-Dockum palaeoriver system. *Science*, 273: 97–100.

Rosell, J. & Obrador, A., 1982. Oncolites from lacustrine sediments in the Cretaceous of north-eastern Spain. *Sedimentology*, 29: 433–436.

Rowe, C. M., Loope, D. B., Oglesby, R. J., Van der Voo, R. & Broadwater, C. E., 2007. Inconsistencies between Pangean reconstructions and basic climate controls. *Science*, 318: 1284–1286.

Shankar, N. & Achyuthan, H., 2007. Genesis of calcic and petrocalcic horizons from Coimbatore, Tamil Nadu: Micromorphology and geochemical studies. *Quaternary International*, 175: 140–154.

Shrivastava, P., Bhattacharyya, T. & Pal, D. K., 2002. Significance of the formation of calcium carbonate minerals in the pedogenesis and management of cracking clay soils (vertisols) of India. *Clays and Clay Minerals*, 50: 111–126.

Sinclair, A. R. E., Mduma, S. A. R., Hopcraft, J. G. C., Fryxell, J. M., Hilborn, R. & Thirgood, S., 2007. Long-term ecosystem dynamics in the Serengeti: Lessons for conservation. *Conservation Biology*, 21: 580–590.

Slingerland, R. & Smith, N. D., 2004. River avulsions and their deposits. *Annual Review of Earth and Planetary Sciences*, 32: 257–285.

Smith, R. M. H., 1987. Helical burrow casts of therapsid origin from the Beaufort Group (Permian) of South Africa. *Palaeogeography, Palaeoclimatology, Palaeoecology*, 60: 155–170.

Smith, J. J. & Hasiotis, S. T., 2008. Traces and burrowing behaviors of the cicada nymph *Cicadetta calliope*: Neoichnology and palaeoecological significance of extant soil-dwelling insects. *Palaios*, 23: 503–513.

Smith, J. J., Hasiotis, S. T., Kraus, M. J. & Woody, D., 2008a. *Naktodemasis bowni*: new ichnogenus and ichnospecies for adhesive meniscate burrows (AMB), and palaeoenvironmental implications, Paleogene Willwood Formation, Bighorn Basin, Wyoming. *Journal of Paleontology*, 82: 267–278.

Smith, J. J., Hasiotis, S. T., Kraus, M. J. & Woody, D. T., 2008b. Relationship of floodplain ichnocoenoses to palaeopedology, palaeohydrology, and palaeoclimate in the Willwood Formation, Wyoming, during the Paleocene-Eocene Thermal Maximum. *Palaios*, 23: 683–699.

Smith, J. J., Hasiotis, S. T., Woody, D. T. & Kraus, M. J., 2008c. Paleoclimatic implications of crayfish-mediated prismatic structures in palaeosols of the Paleogene Willwood Formation, Bighorn Basin, Wyoming, U.S.A. *Journal of Sedimentary Research*, 78: 323–334.

Smith, J. J., Hasiotis, S. T., Woody, D. T., & Kraus, M. J. 2009. Transient dwarfism of soil fauna during the Paleocene-Eocene Thermal Maximum. *Proceedings of the National Acad-*

emy of Science, Early Edition, www.pnas.org/cgi/doi/10.1073/ pnas.0909674106, p. 1-6, plus supplemental data.

Smith, N. D., Cross, T. A., Dufficy, J. P. & Clough, S. R., 1989. Anatomy of an avulsion. *Sedimentology*, 36: 1–23.

Stanley, K. O. & Fagerstrom. J. A., 1974. Miocene invertebrate trace fossils from a braided river environment, western Nebraska, U.S.A. *Palaeogeography, Palaeoclimatology, Palaeoecology*, 15: 63–82.

Steiner, M. B. & Lucas, S. G., 2000. Paleomagnetism of the Late Triassic Petrified Forest Formation, Chinle Group, western United States: Further evidence of 'large' rotation of the Colorado Plateau. *Journal of Geophysical Research, Series B, Solid Earth and Planets*, 105: 25791–25808.

Stewart, J. H., Anderson, T. H., Haxel, G. B., Silver, L. T. & Wright, J. E., 1986. Late Triassic palaeogeography of the southern Cordillera: The problem of a source for voluminous volcanic detritus in the Chinle Fm of the Colorado Plateau region. *Geology*, 14: 567–570.

Stewart, J. H., Poole, F. G. & Wilson, R. F., 1972. Stratigraphy and origin of the Chinle Fm and related Upper Triassic strata in the Colorado Plateau region. *U. S. Geological Survey Professional Paper,* 690: 1–336.

Stiles, C. A., Mora, C. I. & Driese, S. G., 2001. Pedogenic iron-manganese nodules in vertisols: A new proxy for palaeoprecipitation? *Geology*, 29: 943–946.

Teller, J. T. & Last, W. M., 1990. Paleohydrological indicators in playas and salt lakes, with examples from Canada, Australia, and Africa. *Palaeogeography, Palaeoclimatology, Palaeoecology*, 76: 215–240.

Therrien, F. & Fastovsky, D. E., 2000. Paleoenvironments of early theropods, Chinle Fm (Late Triassic), Petrified Forest National Park, Arizona. *Palaios*, 15: 194–211.

Trendell, A. M., Atchley, S. C. & Nordt, L. C., 2012. Depositional and diagenetic controls on reservoir attributes within a fluvial outcrop analog: Upper Triassic Sonsela Mbr of the Chinle Fm, Petrified Forest National Park, Arizona. *AAPG Bulletin*, 96: 679–707.

Trendell, A. M., Atchley, S. C. & Nordt, L. C., 2013a. Facies analysis of a probable large-fluvial-fan depositional system: The Upper Triassic Chinle Fm at Petrified Forest National Park, Arizona, U.S.A. *Journal of Sedimentary Research*, 83: 873–895.

Trendell, A. M., Nordt, L. C., Atchley, S. C., Leblanc, S. L. & Dworkin, S. I., 2013b. Determining floodplain plant distributions and populations using palaeopedology and fossil root traces: Upper Triassic Sonsela Mbr of the Chinle Fm at Petrified Forest National Park, Arizona. *Palaios*, 28: 471–490.

Turner, B. R., 1993. Paleosols in Permo-Triassic continental sediments from Prydz Bay, East Antarctica. *Journal of Sedimentary Petrology*, 63: 694–706.

Van der Voo, R., Mauk, F. J. & French R. B., 1976. Permian-Triassic continental configurations and the origin of the Gulf of Mexico. *Geology*, 4: 177–180.

van der Kolk, D. A., Flaig, P. P. & Hasiotis, S. T., 2015. Paleoenvironmental reconstruction of a Late Cretaceous, muddy, river-dominated polar deltaic system: Schrader Bluff-Prince Creek Formation transition, Shivugak Bluffs, North Slope of Alaska, U.S.A. *Journal of Sedimentary Research*, 85: 903–936.

Vittum, P. J., Villani, M. G. & Tahiro, H., 1999. *Turfgrass Insects of the United States and Canada, 2nd Edition*. Cornell University Press, Ithaca, 422 pp.

Wallace, J. B. & Merritt, R. W., 1980. Filter-feeding ecology of aquatic insects. *Annual Review of Entomology*, 25: 103– 32.

Zeigler, K. E. & Geissman, J. W., 2011. Magnetostratigraphy of the Upper Triassic Chinle Group of New Mexico: Implications for regional and global correlations among Upper Triassic sequences. *Geosphere*, 7: 802–829.